

FLOTATION OF HALITE AND SYLVITE FROM CARNALLITE  
WITH DODECYL MORPHOLINE

by

Bo Pan

A thesis submitted to the faculty of  
The University of Utah  
in partial fulfillment of the requirements for the degree of

Master of Science

Department of Metallurgical Engineering

The University of Utah

F gego dgt 2013

Copyright © Bo Pan 2013

All Rights Reserved

# The University of Utah Graduate School

## STATEMENT OF THESIS APPROVAL

The thesis of Bo Pan

has been approved by the following supervisory committee members:

Jan D. Miller, Chair June 21, 2012  
Date Approved

Xuming Wang, Member June 21, 2012  
Date Approved

Michael L. Free, Member June 21, 2012  
Date Approved

and by Jan D. Miller, Chair/Dean of

the Department/College/School of Metallurgical Engineering

and by David B. Kieda, Dean of The Graduate School.

## **ABSTRACT**

Carnallite recovery by reverse flotation of halite with dodecyl morpholine (DDM) as collector has been applied in industry. Despite successful use in industry, the surface chemistry for halite flotation with DDM collector is not clear. Therefore the major objective of this thesis research was to examine the flotation chemistry in detail and understand the nature of the interaction between the DDM collector and the soluble salt minerals, halite (NaCl), sylvite (KCl), and carnallite ( $\text{KMgCl}_3 \cdot 6\text{H}_2\text{O}$ ).

After the introduction in Chapter 1, the flotation response of halite, sylvite and carnallite is reported as evaluated using microflotation. The results indicate that both NaCl and KCl can be floated using DDM as a collector from saturated solution. However, flotation of carnallite was not achieved at these or higher concentrations. FTIR analysis by the DRIFT technique showed that DDM selectively adsorbed at the surface of NaCl and KCl.

In Chapter 3, the chemical features of dodecyl morpholine were evaluated by surface tension measurements for halite-, sylvite-, and carnallite-saturated solutions. The precipitation concentration was determined by turbidity measurements. In addition, the zeta potential of the collector colloid was also determined at different pH values.

In Chapter 4, the wetting characteristics for NaCl, KCl and carnallite are reported.

Contact-angle measurements as a function of DDM concentration indicate that, when the DDM concentration increased to  $2 \times 10^{-6}$  M, an increase in contact angle was observed at the surface of NaCl and KCl. Bubble attachment-time experiments indicate that there is a critical concentration at which effective attachment occurs.

In Chapter 5, initial efforts to study the interfacial water structure using molecular dynamic simulation (MDS) are described. The simulation results indicate that the carnallite surface was completely hydrated. Therefore, the collector molecules or the collector colloid cannot replace interfacial water molecules at the surface of carnallite, and the carnallite particles remain hydrophilic during flotation with DDM. The water residence time at the NaCl surface, about 30 ps, is longer than the water residence time of 20 ps at the KCl surface but very small when compared with that of carnallite. The water residence time at the carnallite surface is longer than the simulation time of the water/carnallite system (1000 ps). This appears to be the major reason that carnallite cannot be floated using DDM or DDA as collector for that matter.

## TABLE OF CONTENTS

ABSTRACT .....	iii
LIST OF TABLES .....	vii
LIST OF FIGURES .....	viii
ACKNOWLEDGMENTS .....	x
Chapters	Page
1. INTRODUCTION .....	1
1.1 Fertilizer and Potash Ore .....	1
1.2 KCl Flotation Chemistry with Amine Collector .....	3
1.3 Reverse Flotation with Morpholine Collector .....	3
1.4 Current Research Status .....	4
1.5 Research Objectives and Thesis Organization .....	10
2. FLOTATION RESPONSE OF HALITE, SYLVITE, AND CARNALLITE .....	11
2.1 Materials and Experimental Method .....	11
2.2 Microflotation Results and Discussion .....	14
2.3 FTIR Analysis of Flotation Products .....	18
2.4 Summary .....	21
3. COLLECTOR CHEMISTRY .....	23
3.1 Introduction .....	23
3.2 Materials and Experimental Methods .....	25
3.2.1 Surface-Tension Measurements .....	25
3.2.2 DDM Precipitation Concentration Determination .....	25
3.2.3 Zeta-Potential Measurements .....	25

3.3	Results and Discussion .....	26
3.3.1	Surface Tension of DDM Solution .....	26
3.3.2	Precipitation of DDM Collector Colloid .....	30
3.3.3	Zeta Potential of DDM Collector Colloid .....	32
3.4	Summary .....	32
4.	WETTING CHARACTERISTICS OF HALITE, SYVITE, AND CARNALLITE SURFACES .....	35
4.1	Introduction .....	35
4.2	Material and Experimental Methods .....	37
4.2.1	Contact-Angle Measurements .....	37
4.2.2	Bubble Attachment Time .....	38
4.3	Results and Discussion .....	40
4.3.1	Contact-Angle Measurements .....	40
4.3.2	Bubble Attachment Time .....	44
4.4	Summary .....	48
5.	MOLECULAR DYNAMIC SIMULATIONS OF INTERFACIAL WATER AT SYLVITE, HALITE, AND CARNALLITE SURFACES .....	49
5.1	Introduction .....	49
5.2	Molecular Dynamics Simulations .....	50
5.3	Water Density Distributions at NaCl, KCl, and Carnallite Surfaces .....	51
5.4	Water Residence Times at Salt Surfaces .....	57
5.5	Summary .....	59
6.	SUMMARY AND CONCLUSIONS .....	60
	REFERENCES .....	63

## LIST OF TABLES

<u>Table</u>	<u>Page</u>
1. 1 World Mine Production and Reserves (Adapted from USGS, 2012) .....	2
1. 2 Heat of Solution $H_s$ (kcal mole <sup>-1</sup> ) at Infinite Dilution for Monovalent Halite Salts at 18°C (Adapted from Roger and Schulman, 1957).....	8
2. 1 Observations for Flotation of Halite, Sylvite, and Carnallite in Saturated Brines Using DDM and DDA as Collectors .....	17
2. 2 Error Calculation for KCl Flotation with Dodecyl Morpholine at a Concentration of $1 \times 10^{-5}$ M.....	18
3. 1 Properties of Dodecyl Morpholine.....	24
3. 2 Saturated Salt Solutions, Concentration, Ionic Strength, Surface Tension, and DDM Precipitation Concentration at 23.5°C (Adapted from Hancer and Miller, 2000).....	30
5. 1 Salt Parameters for Molecular Dynamics Simulations .....	51
5. 2 Water Residence Times at Water/Salt Interfaces.....	59



## LIST OF FIGURES

<b><u>Figure</u></b>	<b><u>Page</u></b>
1.1 Flow sheet for reverse flotation of carnallite ore .....	5
1.2 Collector adsorption mechanism according to the ion exchange model. Exchange of the long-chain amine at the surface of KCl and NaCl; the smaller surface lattice space for Na <sup>+</sup> does not allow for long-chain amine substitution. ....	6
2.1 Micro-flotation experimental apparatus .....	13
2.2 Flotation results from micro-flotation experiments for halite, sylvite, and carnallite in saturated brines using DDA as collector (particle size: 70 × 100 mesh) .....	15
2.3 Flotation results from micro-flotation experiments for halite, sylvite, and carnallite in saturated brines using DDM as collector (particle size: 70 × 100 mesh) .....	16
2.4 The transmission FTIR of DDM collector .....	19
2.5 FTIR spectra for halite flotation products with DDM as collector .....	20
2.6 FTIR spectra for sylvite flotation concentrate with DDM as collector .....	22
3.1 Structure of alkyl-morpholine molecule .....	23
3.2 The surface tension for DDM in an NaCl-saturated solution.....	27
3.3 The surface tension for DDM in a KCl-saturated solution .....	28
3.4 The surface tension for DDM in a carnallite-saturated solution .....	29
3.5 The turbidity adsorbance of DDM in saturated solutions of KCl, NaCl, and carnallite. ....	31

3.6	Zeta potential of DDM colloid in DI-water as a function of pH.....	33
4.1	Schematic of a sessile-drop contact angle.....	36
4.2	Schematic of MCT-100 Electronic Induction Timer.....	38
4.3	Attachment event.....	39
4.4	Contact angle at an NaCl surface in DDM solution as a function of DDM concentration... ..	41
4.5	Contact angle at a KCl surface in DDM solution as a function of DDM concentration... ..	42
4.6	Contact angle at NaCl and KCl surfaces in DDA solution as a function of DDA concentration... ..	43
4.7	Bubble attachment-time results for NaCl in DDM solutions of different concentrations.....	45
4.8	Bubble attachment-time results for KCl in DDM solutions of different concentrations.....	46
4.9	Bubble attachment-time results for carnallite in DDM solutions of different concentrations.....	47
5.1	Close-up MDS snapshots of water molecules near KCl and NaCl surfaces, taken at the equilibrium state (1 ns) .....	52
5.2	Close-up MDS snapshot of water molecules near a carnallite surface, taken at the equilibrium state (1 ns)... ..	53
5.3	Water density profile at the water/NaCl interface ... ..	54
5.4	Water density profile at the water/KCl interface ... ..	55
5.5	Water density profiles at the water/carnallite interface .....	56
5.6	Water residence times at the water/NaCl and water/KCl interfaces .....	58

## **ACKNOWLEDGMENTS**

I would like to thank my supervisor, Professor J. D. Miller, for his invaluable personal and technical advice and guidance which allowed the successful completion of this thesis research and my academic education. Thanks are extended to members of my supervisory committee, Dr. Xuming Wang and Dr. Michael L. Free, for their suggestions and guidance.

Thanks to Jiaqi Jin for his assistance in MDS simulation. Also thanks are given to Professor Fanqing Cheng at Shanxi University in China for her valuable discussion and encouragement. Further appreciation is extended for assistance from my colleagues, staff, and other faculty members.

Financial support for this research was provided by the University of Utah and is gratefully recognized.

Finally, sincere appreciation is expressed to my parents for their understanding and support.

# **CHAPTER 1**

## **INTRODUCTION**

### **1.1 Fertilizer and Potash Ore**

Potassium is one of the three basic plant nutrients, along with nitrogen and phosphorus. There are no substitutes for potassium as an essential nutrient for plants, animals, and humans (U.S. Geological Survey, 2012). About 95% of potash produced worldwide is used in agriculture. It is essential to maintain and expand food production. The rest of the potash produced is used in glass manufacturing, plastics, and pharmaceuticals (Perucca, 2003). World consumption of potash is projected to increase about 4% annually during the next five years due to world population growth and the concurrent need for increased production of food and biofuels (U.S. Geological Survey, 2012).

As shown in Table 1.1, major production is from Canada, Russia and Belarus. World production of potash has increased and will continue to increase for the next decade, with significant additions to capacity planned in Argentina, Belarus, Canada, Congo (Brazzaville), and the United Kingdom (U.S. Geological Survey, 2012).

Potash is extracted from the earth by underground or solution mining. Over 50 million tons of sylvite ( $\text{KCl}$ ) is produced annually from potash ore, primarily by the flotation process. Flotation involves the use of long-chain primary amines as collector for the flotation of  $\text{KCl}$  from  $\text{NaCl}$  and  $\text{MgCl}_2$  (Cao, 2010).

Table 1.1 World Mine Production and Reserves (Adapted from USGS, 2012)

Country	2010	2011	Reserves
United states	930	1100	130,000
Belarus	5,250	5,500	750,000
Brazil	453	400	300,000
Canada	9,788	11,200	4,400,000
Chile	800	800	130,000
China	3,200	3,200	210,000
Germany	3,000	3,300	150,000
Israel	1,960	2,000	740,000
Jordan	1,200	1,400	740,000
Russia	6,280	7,400	3,300,000
Spain	415	420	20,000
United Kingdom	427	430	22,000
other	---	----	50,000
World total	33,700	37,000	9,500,000

\*Data in thousand metric tons of K<sub>2</sub>O equivalent

## 1.2 KCl Flotation Chemistry with Amine Collector

Currently, over 80% of the world's potash is produced by the selective flotation of KCl (sylvite) from NaCl (halite) and other gangue minerals using long-chain amine collectors that generally contain from 16 to 22 carbon atoms in the aliphatic chain. Other reagents including slime depressants, dispersants, and frothers are also used to improve the efficiency of the amine flotation process (Searls, 1990).

Motivated by the successful development of KCl flotation by industry, significant research has been directed to understand the difference in flotation behavior between structurally similar sylvite and halite when long-chain amines are used as collectors. A number of models have been proposed to explain the adsorption states of selected surfactant molecules at alkali halide salt surfaces: an ion exchange model (Fuerstenau and Fuerstenau, 1956), a heat of solution model (Rogers, 1957; Rogers and Schulman, 1957), a surface charge model (Miller et al., 1992; Roman et al., 1968; Yalamanchili et al., 1993), and an interfacial water structure model (Du and Miller, 2007; Du et al., 2008; Hancer et al., 2001; Hancer and Miller, 2000). The issue of amine collector colloids precipitation and its significance, mentioned by Fuerstenau and Fuerstenau (1956) and cited by Miller et al. (1993), was discussed further by Laskowski et al. (2008) and found to be a very important consideration.

## 1.3 Reverse Flotation with Morpholine Collector

In some cases carnallite ( $\text{KCl} \cdot \text{MgCl}_2 \cdot 6\text{H}_2\text{O}$ ) is concentrated by reverse flotation and used as a raw material to produce sylvite (KCl) by cold decomposition, with formation of  $\text{MgCl}_2$  in solution and KCl as a solid phase. At present this reverse flotation method is being implemented industrially at the Dead Sea in Israel and Jordan, Chaerhan

Salt Lake in China, and Verkhnekamskoye in Russia. In practice, carnallite ore usually contains a certain amount of halite (NaCl 15-30%), small quantities of sylvite, and water-insoluble clay (Laskowski et al., 2008). The carnallite ore must be concentrated since the cold decomposition process usually requires less than 4 to 6% of halite (Laskowski et al., 2008). Therefore removal of halite from carnallite ore is necessary prior to decomposition. In this regard, a flotation technology has been developed using alkyl-morpholines as collector to float halite and sylvite from carnallite (see Figure 1.1).

Carnallite recovery by reverse flotation of NaCl with alkyl-morpholines as collector has been applied in industry including operations at the Dead Sea, Israel and Jordan; Verkhnekamskoye, Russia; and Chaerhan Salt Lake Group, Qinghai province, China. At Chaerhan Salt Lake, the processing strategy is reverse flotation with dodecyl morpholine followed by cold decomposition and crystallization. The flotation feed particle size is about  $20 \times 80$  mesh and the dodecyl morpholine usage is about 200 to 300 g/t. The production was about 2.5 million tons in 2011.

#### **1.4 Current Research Status**

Flotation chemistry for soluble salt flotation has been studied by many researchers (Titkov et al., 2003). Most research is focused on understanding the mechanism of long-chain amine adsorption at the sylvite (KCl) mineral surface. Many theories and/or models have been proposed.

The ion exchange model (Fuerstenau and Fuerstenau, 1956) explains that the selective adsorption of amine at the sylvite surface is due to the fact that the  $\text{RNH}_3^+$  collector ions can fit into the  $\text{K}^+$  surface sites of the KCl lattice (Figure 1.2). In contrast, the  $\text{RNH}_3^+$  cannot fit into the NaCl lattice (Fuerstenau and Fuerstenau, 1956).

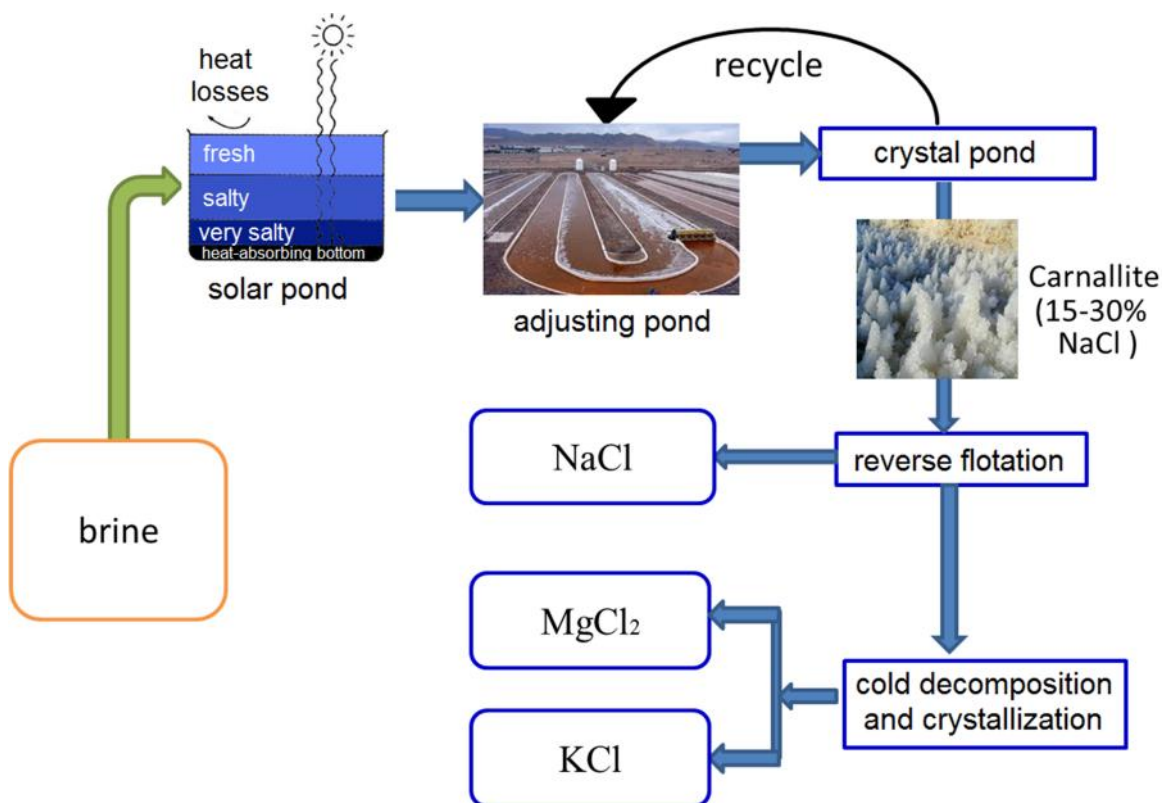


**Figure 1.1** Flow sheet for reverse flotation of carnallite ore.



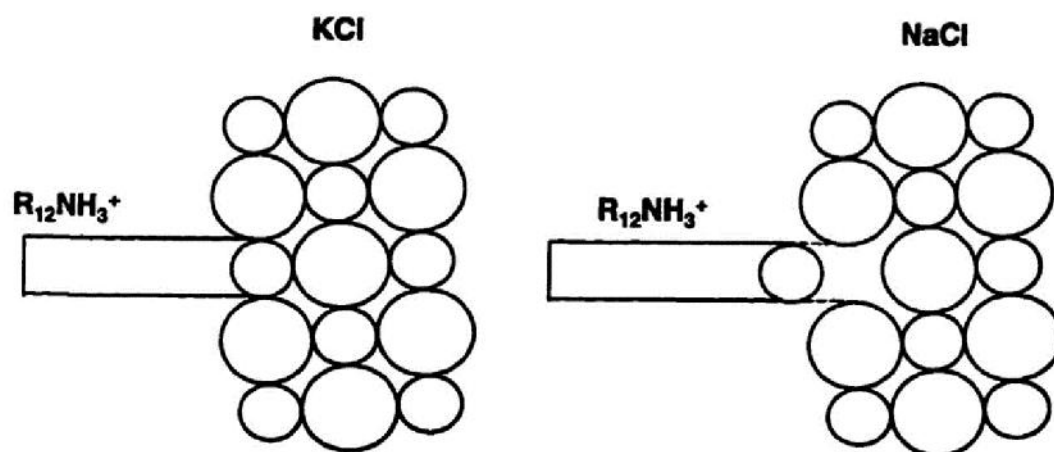


**Figure 1.2** Collector adsorption mechanism according to the ion exchange model. Exchange of the long-chain amine at the surface of KCl and NaCl; the smaller surface lattice space for  $Na^+$  does not allow for long-chain amine substitution.

Further, it is expected that only those minerals with a cation of a size similar to  $\text{RNH}_3^+$  can be floated with amine collectors (Fuerstenau and Fuerstenau, 1956), although several exceptions to this theory are reported (Roman et al., 1968).

The heat of solution model (Roger and Schulman, 1957) considers that only weakly hydrated salt minerals can be floated with DDA. Some strongly hydrated salts can also be floated. However, excessively hydrated salt minerals cannot be floated at all. Rogers and Schulman summarized the heat of solution values for the 24 monovalent halide salts, as shown in Table 1.2. The selective adsorption of amine at a salt surface can be explained based on the heat of solution of a given salt, if positive, no collector adsorption occurs and no flotation is possible. However, adsorption and flotation will occur whenever the heat of solution is sufficiently negative.

According to the surface charge model (Miller et al., 1992), the governing mechanism for soluble salt flotation is electrostatic interaction between the salt surface and collector species (Roman et al., 1968). The cation amine collector is adsorbed by electrostatic attractive force due to the fact that the sylvite mineral surface has a negative charge as determined using nonequilibrium laser-Doppler velocimetry.

The interfacial water structure model (Hancer and Miller, 2001) suggests that a salt may be classified either as a water structure maker or a water structure breaker, based on the analysis of salt hydration and solution viscosity measurements. A water-structure-maker salt interacts strongly with water molecules, while water-structure-breaker salts have a tendency to break the structure of water at the salt surface. This analysis can be correlated with heat of solution values. Thus a collector molecule can easily replace the water molecule at the surface of a water-structure-breaker salt.

**Table 1.2** Heat of Solution  $H_s$  (kcal mole<sup>-1</sup>) at Infinite Dilution for Monovalent Halite Salts at 18°C (Adapted from Roger and Schulman, 1957)

	Li <sup>+</sup>	Na <sup>+</sup>	K <sup>+</sup>	Rb <sup>+</sup>	Cs <sup>+</sup>	NH <sub>4</sub> <sup>+</sup>
F <sup>-</sup>	-1.0					-1.5
Cl <sup>-</sup>			-3.8	-4.2	-3.9	-3.4
Br <sup>-</sup>		-4.6	-4.1	-5.9	-6.6	-4.5
I <sup>-</sup>		-3.9	-3.4	-6.3	-8.1	-3.6

From the ion exchange theory, KCl can be floated with amines as collector because the head group of collector ions can fit into the  $K^+$  surface sites of the KCl lattice. In contrast,  $RNH_3^+$  cannot fit into the NaCl lattice (Fuerstenau and Fuerstenau, 1956). However, this theory cannot explain why alkyl sulfate can be used to float KCl (Hancer et al., 2001) nor why long-chain morpholine collectors can float both sylvite and halite.

According to the interfacial water structure model, KCl is a water-structure-breaker salt, while NaCl is a water-structure-maker salt; therefore adsorption occurs at the KCl surface. In this regard, the theory of interfacial water structure does not explain the adsorption of dodecyl morpholine at the NaCl surface. As mentioned above, nonequilibrium electrophoretic mobility measurements (Miller et al., 1992) show that KCl and NaCl have opposite surface charges, but both KCl and NaCl can be floated using DDM as collector. It appears that the surface charge model cannot explain the adsorption behavior of DDM at KCl and NaCl surfaces.

Despite successful use in industry, there is still little research reported on DDM flotation. Titkov et al. (2003) investigated the flotation of NaCl and KCl from carnallite using alkylmorpholine as collector. The flotation results indicate that alkylmorpholine can be used to selectively float halite from carnallite mixtures. In this study different chain lengths of alkyl morpholine were evaluated, and the results indicated that the flotation activity of alkylmorpholine mixtures is much higher than that of a single alkylmorpholine compound. The addition of frother increased the adsorption of alkylmorpholine at the halite surface and reduced the morpholine consumption

The flotation behavior of halite was studied using DDM as a collector by Zhang and Song (2006). They tried to explain the adsorption mechanism, but the conclusions

were uncertain. They made the same observation as Titkov et al. (2003), that the addition of frother increased the adsorption density.

Despite successful plant practice to separate halite from carnallite using DDM, the mechanism of adsorption of DDM at the halite surface is still unclear. Therefore, it is desired to understand the fundamental flotation behavior using DDM as collector. In this regard this thesis research program was organized to establish basic understanding of the use of DDM as a collector in the flotation of halite and sylvite from carnallite.

### **1.5 Research Objectives and Thesis Organization**

The surface chemistry for halite flotation with DDM as collector is not clear. There is little fundamental information in the literature about the flotation of halite with DDM. Therefore, the major objective of this research was to determine the flotation chemistry in greater detail and understand the nature of the interaction between the DDM collector and halite. Based on experimental results, the following thesis organization was prepared.

1. Introduction including review of the literature, Chapter 1.
2. Microflotation response of halite, sylvite and carnallite, Chapter 2.
3. Collector chemistry including DDM precipitation, Chapter 3.
4. Wetting characteristics of halite, sylvite and carnallite surfaces, Chapter 4.
5. Preliminary structure of interfacial water at halite, sylvite and carnallite surfaces as revealed from molecular dynamics simulations (MDS), Chapter 5.
6. Summary and conclusions, Chapter 6.

## **CHAPTER 2**

### **FLOTATION RESPONSE OF HALITE, SYLVITE, AND CARNALLITE**

In this chapter, micro-flotation experiments were carried out to evaluate the flotation response for halite, sylvite, and carnallite with dodecyl amine hydrochloride (DDA) and dodecyl morpholine (DDM) as collectors.

#### **2.1 Materials and Experimental Method**

Dodecyl amine hydrochloride (DDA) with a purity of 99.0% was purchased from ACROS. The reagent was used as received and without further purification. Freshly made  $1 \times 10^{-2}$  mol/L of DDA stock solution was prepared and a carefully calculated amount was added to the brine to obtain the desired surfactant concentration.

A reagent-grade 4-dodecyl morpholine-4-hydrochloride (DDM) with a purity of 99.5% was purchased from Sigma-Aldrich, ACS. The reagent was used as received and without further purification. Freshly made  $1 \times 10^{-2}$  mol/L DDM stock solution was prepared, and a carefully calculated amount was added to the brine to obtain the desired surfactant concentration.

Carnallite was obtained from Catic's Meihai operation in China and confirmed by XRD. KCl and NaCl crystals were obtained from International Crystal Laboratories. All materials were used as received and without further purification. Chemical Millipore

(Milli Q, Millipore Corp, 18M ) water was used in all experiments.

Saturated brines were prepared by dissolution of a sufficient amount of salt in DI water with stirring for 24 hours. Then the saturated solutions were stored at room temperature overnight and filtered before use. The presence of salt crystals was indicative of brine saturation.

The flotation experiments were conducted in a 125-ml flotation column ( $20 \times 220$  mm) with a fine frit (10  $\mu$ m) and a magnetic stirrer. The experimental setup is shown in Figure 2.1. Salt samples (70  $\times$  100 mesh) of 2 g were used in each microflotation test. A saturated solution containing the desired collector was first conditioned for 15 min and then an additional 8 min after addition of the 2-g salt sample. The samples were floated for 1 min at an air flow rate of 50 cm<sup>3</sup> per min. The float and sink products were filtered, dried and weighed to determine the flotation recovery of the mineral being studied.

The FTIR drift method was used to detect collector adsorption. Diffuse reflectance occurs when light impinges on the surface of a material and is partially reflected and partially transmitted. Light that passes into the material may be absorbed or reflected out again. Hence, the radiation that reflects from an absorbing material is composed of surface-reflected and bulk re-emitted components, which when summed together are the diffuse reflectance of the sample. In this research FTIR spectroscopy was used to examine the adsorption of DDM. Powder samples of flotation products (float and sink) were examined using the drift method. The samples were ground using a mortar and directly filled into the sample holder without any dilution.

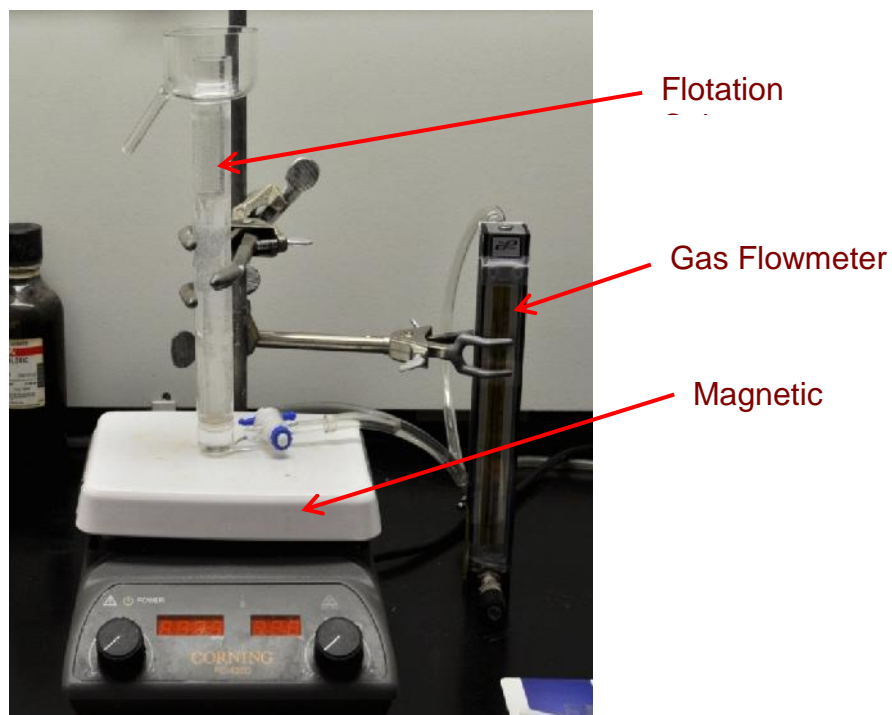


Figure 2.1 Micro-flotation experimental apparatus.



## 2.2 Microflotation Results and Discussion

As shown in Figure 2.2, in the amine flotation system the KCl can be floated with DDA (amine) collector but NaCl and carnallite cannot be floated with amine collector. Further, with an increase in collector concentration, the flotation recovery increases monotonically, and nearly 100% KCl recovery is achieved at  $2 \times 10^{-3}$  M DDA. The flotation behavior of KCl appears to be dependent on the interfacial water structure at the salt surface, KCl being a water-structure-breaking salt. On the other hand, no significant flotation is observed for water-structure-maker salts, NaCl and carnallite, even at high DDA concentrations. The flotation results suggest that the hydration state of the salt surface is an important surface feature for determining the flotation response. Precipitation of DDA must also be considered.

The flotation response is much different with DDM as collector. Shown in Figure 2.3 are the results from microflotation experiments for KCl, NaCl, and carnallite in each of their saturated brines using DDM as collector. It can be seen that both the NaCl and the KCl can be effectively floated by DDM when the DDM concentration is greater than  $3 \times 10^{-6}$  M. It seems evident that DDM is a much stronger collector than DDA (see Table 2.1). The flotation recovery increases with an increase in DDM concentration increase. When the DDM concentration is at  $1 \times 10^{-4}$  M, a flotation recovery of 90% can be achieved. On the other hand, the carnallite cannot be floated at these concentrations. It appears that a slightly higher flotation recovery can be achieved for NaCl than for KCl.

It is interesting to note that, in both amine flotation and morpholine flotation systems, flotation occurred when the collector concentration reached a certain critical point. For example, in amine flotation, when the DDA concentration is less than  $5 \times 10^{-5}$  M,

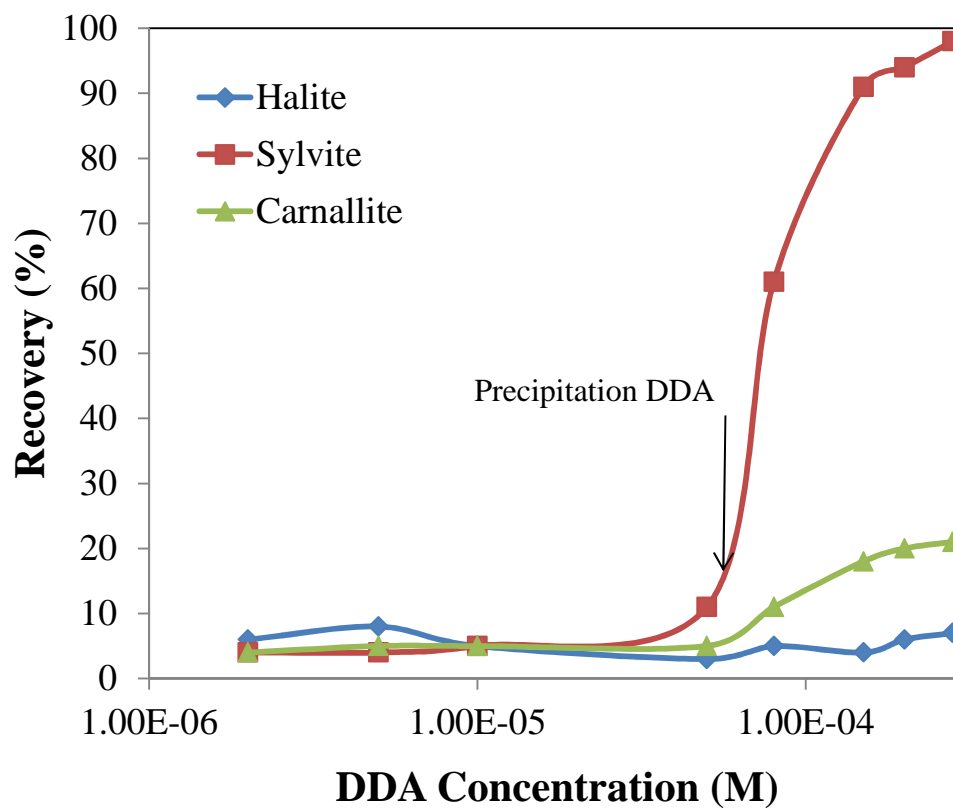


Figure 2.2 Flotation results from micro-flotation experiments for halite, sylvite, and carnallite in saturated brines using DDA as collector (particle size:  $70 \times 100$  mesh).

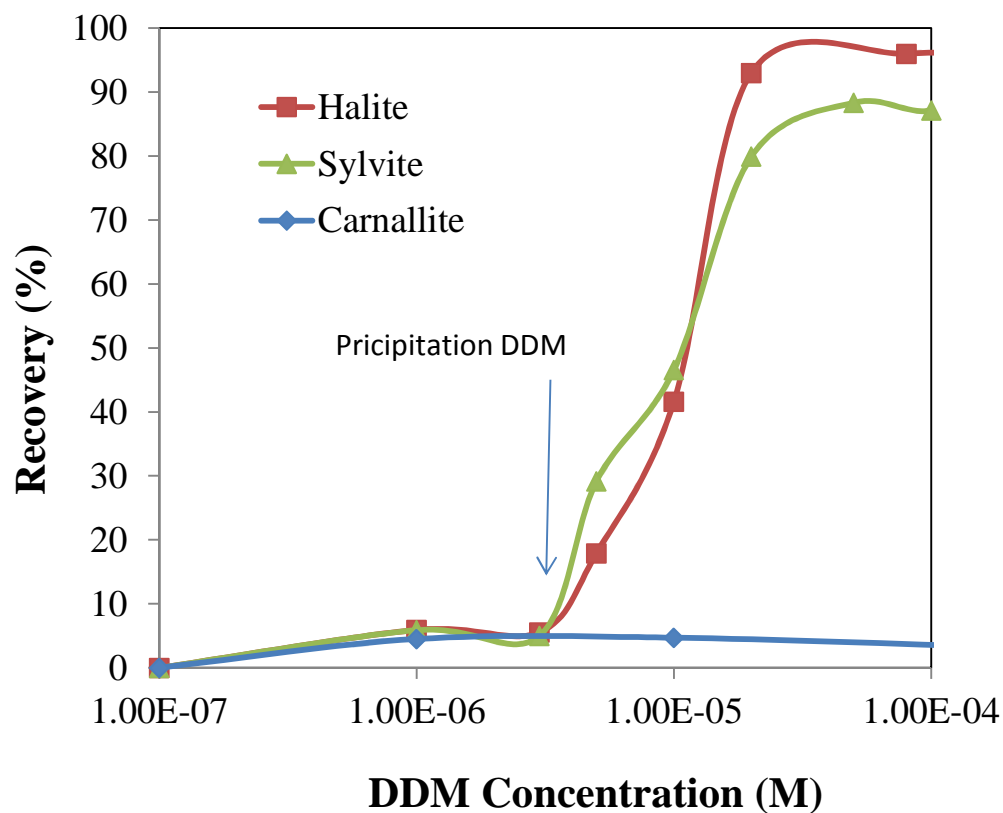


Figure 2.3 Flotation results from micro-flotation experiments for halite, sylvite, and carnallite in saturated brines using DDM as collector (particle size:  $70 \times 100$  mesh).

Table 2.1 Observations for Flotation of Halite, Sylvite, and Carnallite in Saturated Brines Using DDM and DDA as Collectors

Collector	Saturated Brine	Flotation Possibility	Colloid Precipitation
DDM	Halide	Yes	Yes
	Sylvite	Yes	Yes
	Carnallite	No	No
DDA	Halide	No	No
	Sylvite	Yes	Yes
	Carnallite	No	No

there is no flotation response. In the case of the morpholine flotation system, when the morpholine concentration is greater than  $3 \times 10^{-6}$  M, the flotation recovery of halite sylvite increased significantly. This critical concentration appears to be related to the collector precipitation concentration in the saturated solution.

The flotation experimental error was also estimated. Four repeat tests were carried out, and the results are listed in Table 2.2. The estimated variance  $S^2$  is about 2.06%.

### 2.3 FTIR Analysis of Flotation Products

Shown in Figure 2.4 is the FTIR transmission spectrum for the DDM collector. The CH stretching modes appear in the range of  $2850 \text{ cm}^{-1}$  to  $3000 \text{ cm}^{-1}$ . The ring structure is characterized by the peaks at  $1440 \text{ cm}^{-1}$ ,  $1638 \text{ cm}^{-1}$  and  $1720 \text{ cm}^{-1}$ .

Figure 2.5 shows the DRIFT spectra for the flotation products. From the spectra it is clearly seen that there are no CH stretching peaks found for the NaCl feed material. This means that the NaCl material is very clean. CH stretching peaks in the range of  $2850 \text{ cm}^{-1}$  to  $3000 \text{ cm}^{-1}$  appear at the NaCl surface (flotation concentrate). CH stretching

Table 2.2 Error Calculation for KCl Flotation with Dodecyl Morpholine at a Concentration of  $1 \times 10^{-5}$  M

Test No	Recovery (%)
1	40.0
2	41.3
3	43.1
4	42.8
Average	41.8
Variance ( $S^2$ )	2.06

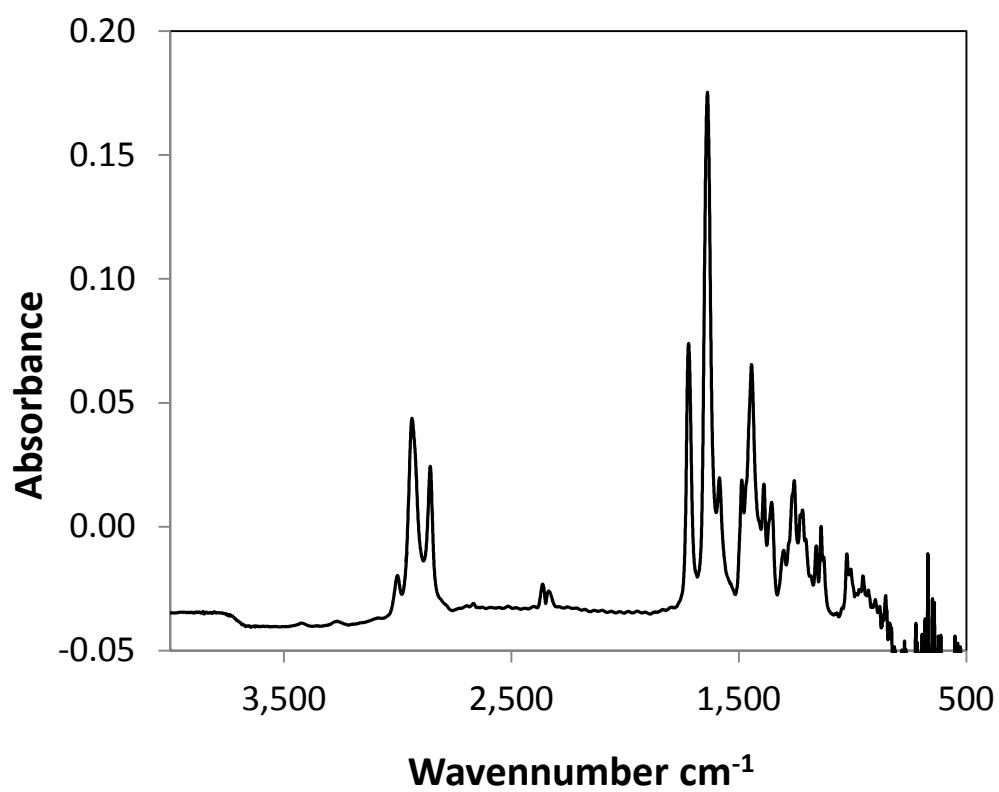


Figure 2.4 The transmission FTIR of DDM collector.

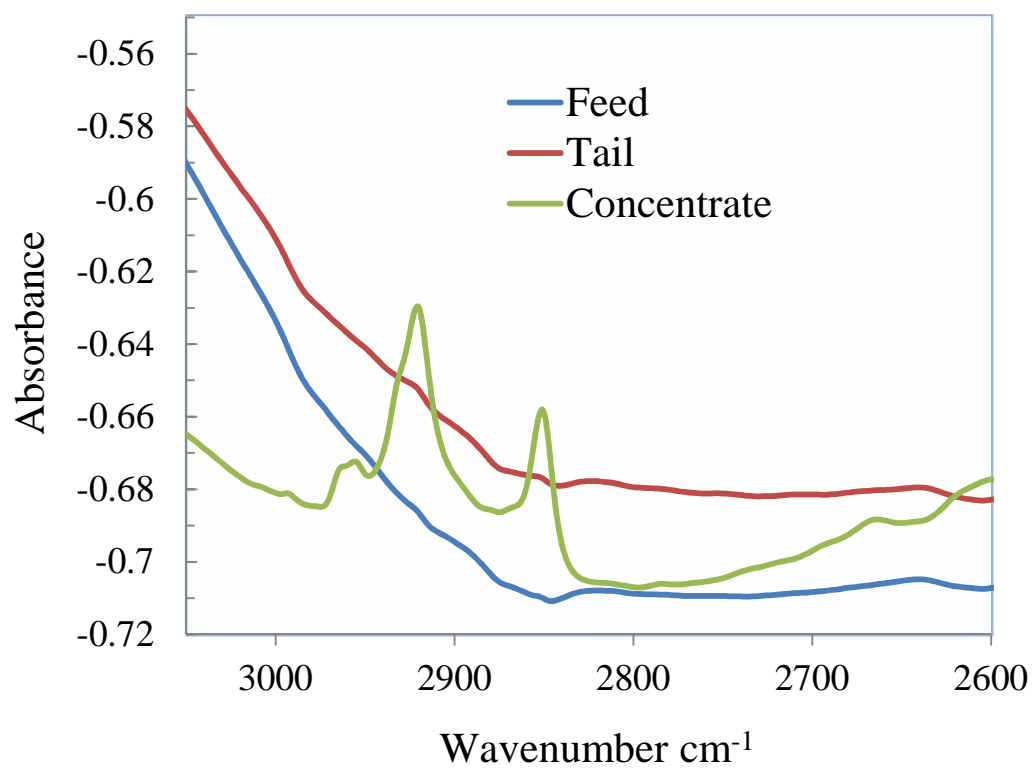


Figure 2.5 FTIR spectra for halite flotation products with DDM as collector.

peaks are also observed for the KCl flotation concentrate as shown in Figure 2.6. No CH stretching peaks were found at the carnallite surface, indicating that DDM adsorption does not occur at the surface of carnallite.

## 2.4 Summary

Both NaCl and KCl can be effectively floated with DDM when the collector concentration is greater than  $3 \times 10^{-6}$  M. The flotation recovery increases with an increase in the DDM concentration. When the DDM concentration reaches  $5 \times 10^{-5}$  M, a flotation recovery of 90% can be achieved. On the other hand, carnallite ( $\text{KMgCl}_3 \cdot 6\text{H}_2\text{O}$ ) cannot be floated even at higher collector concentrations.

The flotation response with DDM is much different from that of flotation with DDA collector. In the DDA amine flotation system, only KCl can be floated at a concentration of  $2 \times 10^{-4}$  M, as required to reach 90% recovery. Neither NaCl nor carnallite can be floated with the amine collector, DDA.

Results also indicate that flotation occurs at a critical collector concentration for both the amine and morpholine flotation systems.

From FTIR spectra analysis, it was found that DDM collector is adsorbed at both the KCl and NaCl surfaces but not at the carnallite surface.



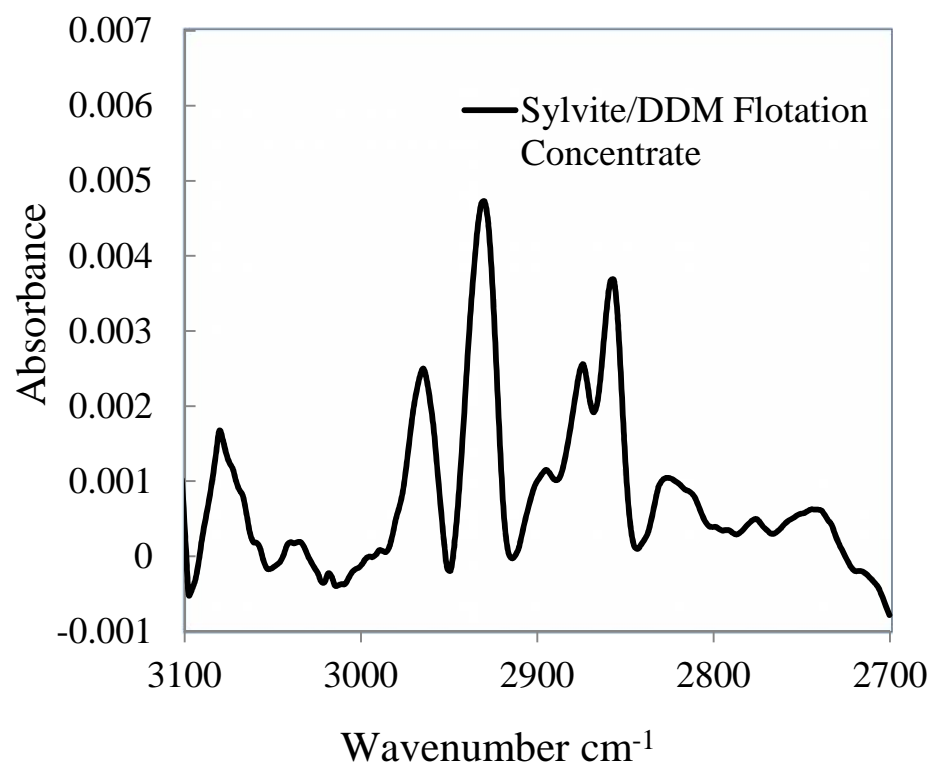


Figure 2.6 FTIR spectra for sylvite flotation concentrate with DDM as collector.

## CHAPTER 3

### COLLECTOR CHEMISTRY

#### 3.1 Introduction

When morpholine is used as the flotation collector, usually an alkyl-morpholine with a 12- to 22-carbon chain is used. A schematic drawing of the alkyl-morpholine molecule is shown in Figure 3.1. The properties of morpholine are similar to those of tertiary amines and are presented in Table 3.1.

Alkyl-morpholines are the products of morpholine and alkyl bromodecane synthesis. Currently dodecyl morpholine is synthesized by the Charerhan Salt Lake Group in China according to the following method:

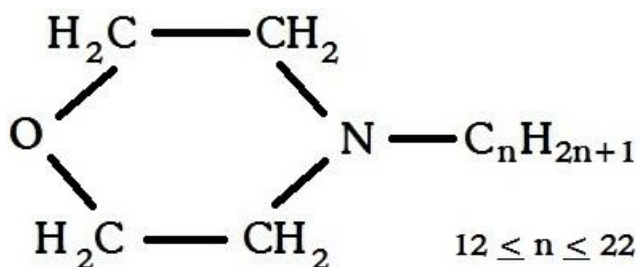
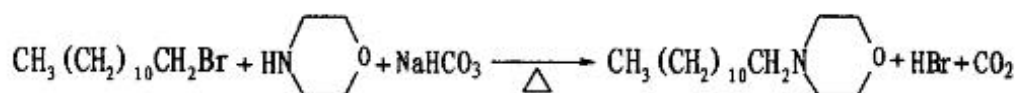


Figure 3.1 Structure of alkyl-morpholine molecule.

Table 3.1 Properties of Dodecyl Morpholine

Formula	C <sub>16</sub> H <sub>33</sub> NO
Molar mass	255.44 g/mol
Appearance	White powder
Density	0.877g/cm <sup>3</sup>
Flash point	98.9°C
Boiling point	334.6°C
Solubility in water	Slightly soluble in water

In practice this synthesis pathway has some disadvantages. For example during synthesis large amounts of CO<sub>2</sub> will be release, and the synthesis time is about 12 hours. The efficiency is about 84% (Yu and Song, 2001). In 2001, they developed a new method which gives a more efficient way to produce dodecyl morpholine for flotation plants. It basically divides the above reaction into two steps. The first is to pre-mix the dodecyl-bromodecane and potassium hydroxide, heat to 150°C, and then add morpholine to produce dodecyl morpholine. The synthesis time was reduced to 4 to 6 hours, and the efficiency was increased to 95%.

In these experiments, the reagent, purchased from Sigma Aldrich, was 4-dodecyl morpholine-4-hydrochloride (DDMHCl(s)) with a purity of 99.5%. The reagent presents as the cation DDMH<sup>+</sup> in aqueous solution, as described by the reaction,



## 3.2 Materials and Experimental Methods

### 3.2.1 Surface-Tension Measurements

The surface tensions of DDM brine solutions were measured using the Du Nouy ring method at room temperature (25°C). All the glassware used in these experiments was cleaned with chromic acid and rinsed with DI-water to prevent contamination. The platinum ring (19.45 mm in diameter) was washed with acetone, methanol and DI-water in sequence, followed by flame treatment to remove organic contaminations. For each measurement, 25-ml samples of brines with a known concentration of DDM were used.

### 3.2.2 DDM Precipitation Concentration Determination

The precipitation concentrations of DDM in brine solutions were determined at room temperature (25°C) using a DR/850 colorimeter. Before the experiment, the glassware used was cleaned with chromic acid and rinsed with DI-water to prevent contamination. For each measurement, 20 ml of brine solution with a known concentration of DDM was used.

### 3.2.3 Zeta-Potential Measurements

Zeta-potential measurements were done using a Zetapals instrument by injecting 1 ml of DDM collector solution. The collector DDM solution was prepared by dissolving DDM into DI water. The concentration was approximately  $1.3 \times 10^{-2}$  M. At this concentration some DDM colloids can be observed. Each Zeta potential measurement was made ten times in order to determine the mean value. The pH value was adjusted by 0.1 M HCl solution or by 0.1 M KOH solution.

### 3.3 Results and Discussion

#### 3.3.1 Surface Tension of DDM Solution

Figure 3.2 shows the results from surface-tension measurements for DDM in a NaCl-saturated solution. It can be observed that the surface tension in this solution decreases with an increase in DDM concentration. A minimum plateau point can clearly be seen. This concentration of  $2 \times 10^{-5}$  M could correspond to the precipitation point in a NaCl-saturated solution at a surface tension of 31 mN/m. The results from microflotation of NaCl showed that a NaCl recovery of 80% can be achieved at  $1 \times 10^{-5}$  M. Similar results were obtained for KCl (see Figure 3.3). In a carnallite-saturated solution, the surface tension plateau concentration is much higher at about  $1 \times 10^{-4}$  M (see Figure 3.4). From these results, it is concluded that DDM precipitation in the KCl and NaCl systems is important for flotation.

The results from surface tension measurements for DDM in a KCl-saturated solution are shown in Figure 3.3. It can be seen that the surface tension of a KCl-saturated solution decreases with an increase in the DDM concentration. A minimum plateau in surface tension of 32 mN/m is reached at about  $2 \times 10^{-5}$  M, which could correspond to the precipitation point in a KCl-saturated solution. The results from microflotation for KCl (Figure 2.1) showed that a KCl recovery of 80% can be achieved at  $2 \times 10^{-5}$  M.

From the DDM surface tension measurements it appears that a minimum plateau in surface tension is reached at around  $2 \times 10^{-5}$  M for both KCl- and NaCl-saturated solutions. In the case of DDM in a carnallite-saturated solution, as shown in Figure 3.4, the plateau point is reached at a concentration of about  $2 \times 10^{-4}$  M (ten times greater than in the case of the NaCl and KCl systems), and the plateau surface tension for carnallite brine is about 30.5 mN/m. The results are summarized in Table 3.2.

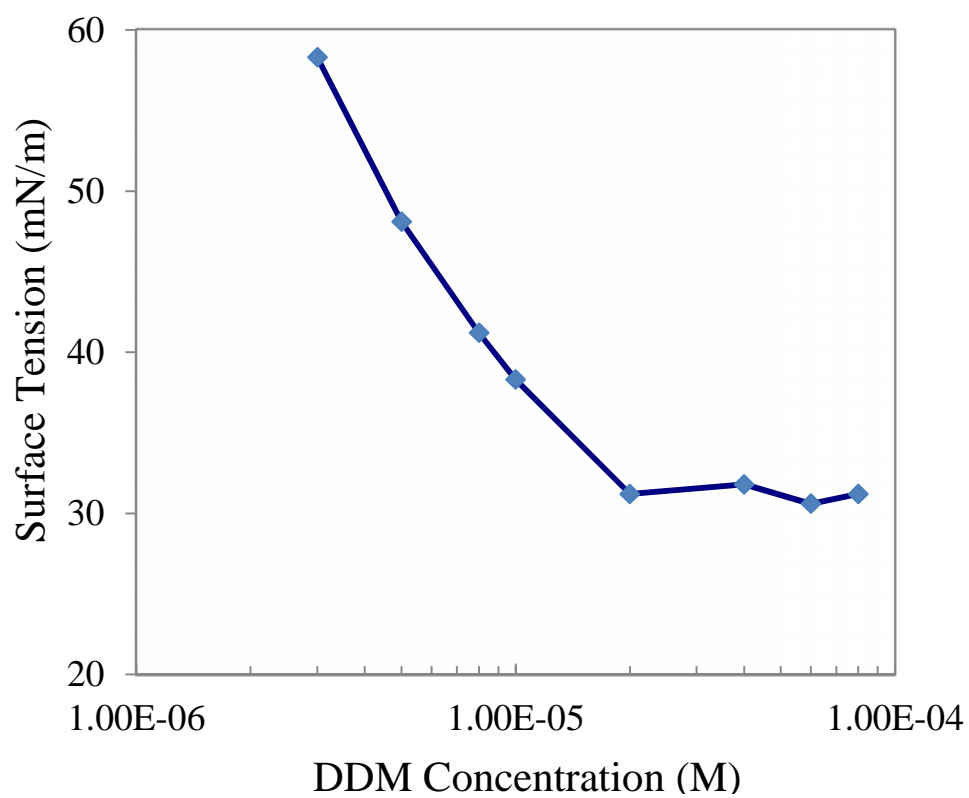


Figure 3.2 The surface tension for DDM in an NaCl-saturated solution.

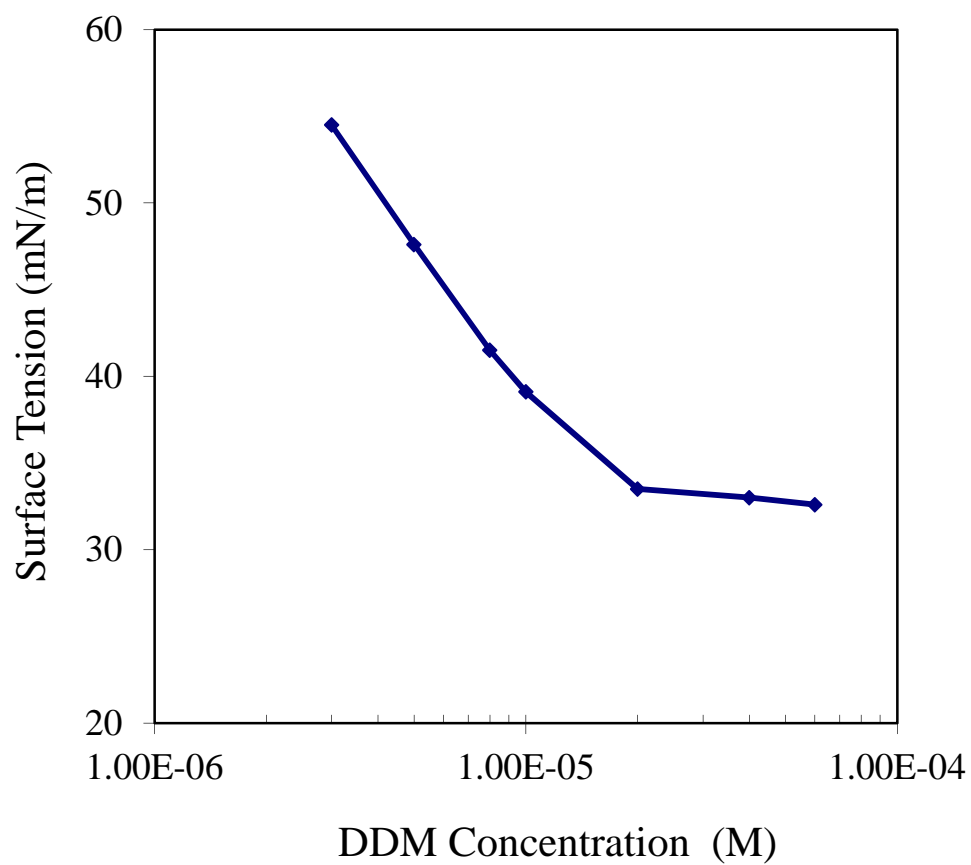


Figure 3.3 The surface tension for DDM in a KCl-saturated solution.

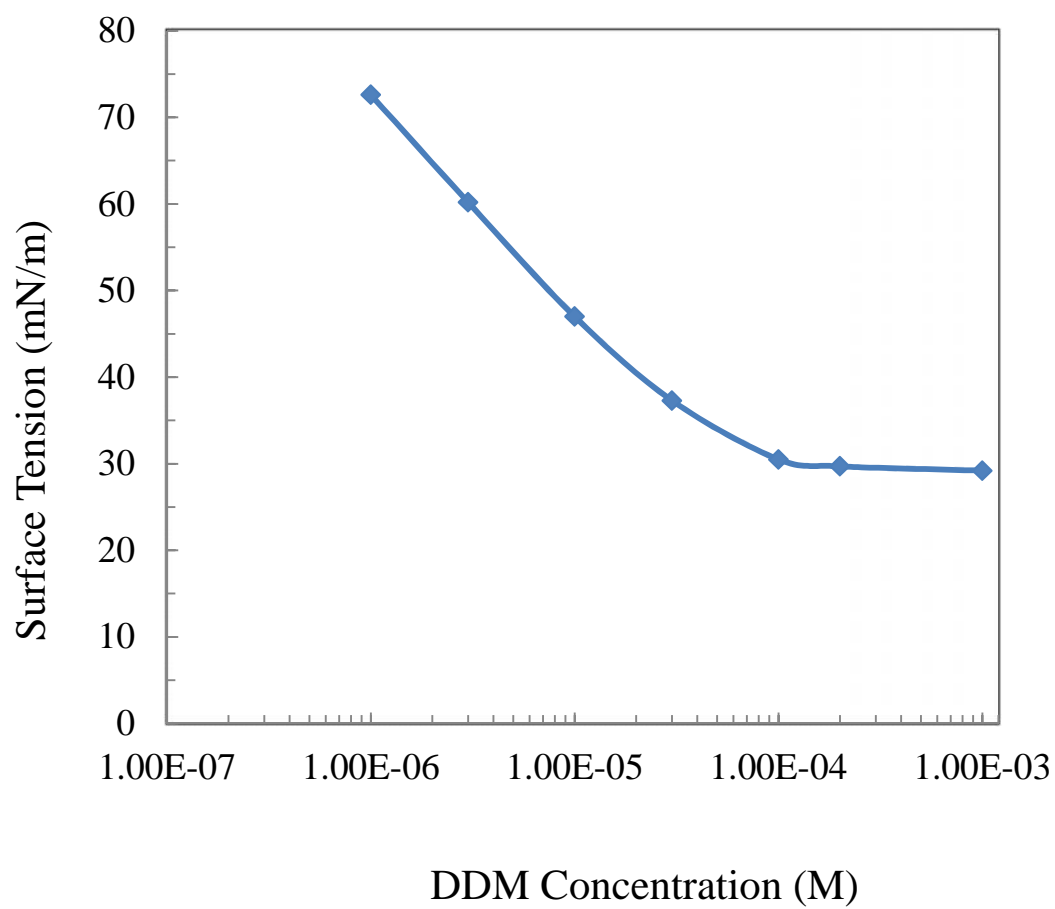


Figure 3.4 The surface tension for DDM in a carnallite-saturated solution.



Table 3.2 Saturated Salt Solutions, Concentration, Ionic Strength, Surface Tension, and DDM Precipitation Concentration at 23.5°C  
(Adapted from Hancer and Miller, 2000)

Salt-saturated brine	Concentration,* M	Ionic strength	Surface tension, mN/m	Precipitation concentration for DDM, M
NaCl	5.1 (NaCl <sub>aq</sub> )	5.1	80.2	$2 \times 10^{-5}$
KCl	4.1 (KCl <sub>aq</sub> )	4.1	76.2	$2 \times 10^{-5}$
KCl·MgCl <sub>2</sub> ·6H <sub>2</sub> O	2.4	9.6	81.3	$1 \times 10^{-4}$

\*The salt concentration from Hancer and Miller (2000)

### 3.3.2 Precipitation of DDM Collector Colloid

If DDM colloid precipitation occurs, the turbidity of the solution will increase. In order to determine the DDM concentration for precipitation of the collector colloid in saturated salt solutions, turbidity at different DDM concentrations was measured. The results, presented in Figure 3.5, show that the turbidity of the DDM solutions starts to change at a concentration of  $2 \times 10^{-5}$  M in NaCl- or KCl-saturated solutions. Combining all the experimental results, it is reasonable to consider the precipitation concentration is in the range of about  $2 \times 10^{-5}$  M in NaCl- or KCl-saturated solutions. In a carnallite-saturated solution, the turbidity transition concentration is about  $1 \times 10^{-4}$  M. This concentration is much higher when compared with the precipitation points in a NaCl- or a KCl-saturated solution. The higher levels of turbidity may indicate the colloid system formed in a NaCl- or KCl-saturated solution exhibits both a smaller particle size and a greater degree of dispersion. In a carnallite-saturated solution, the DDM colloid exhibits

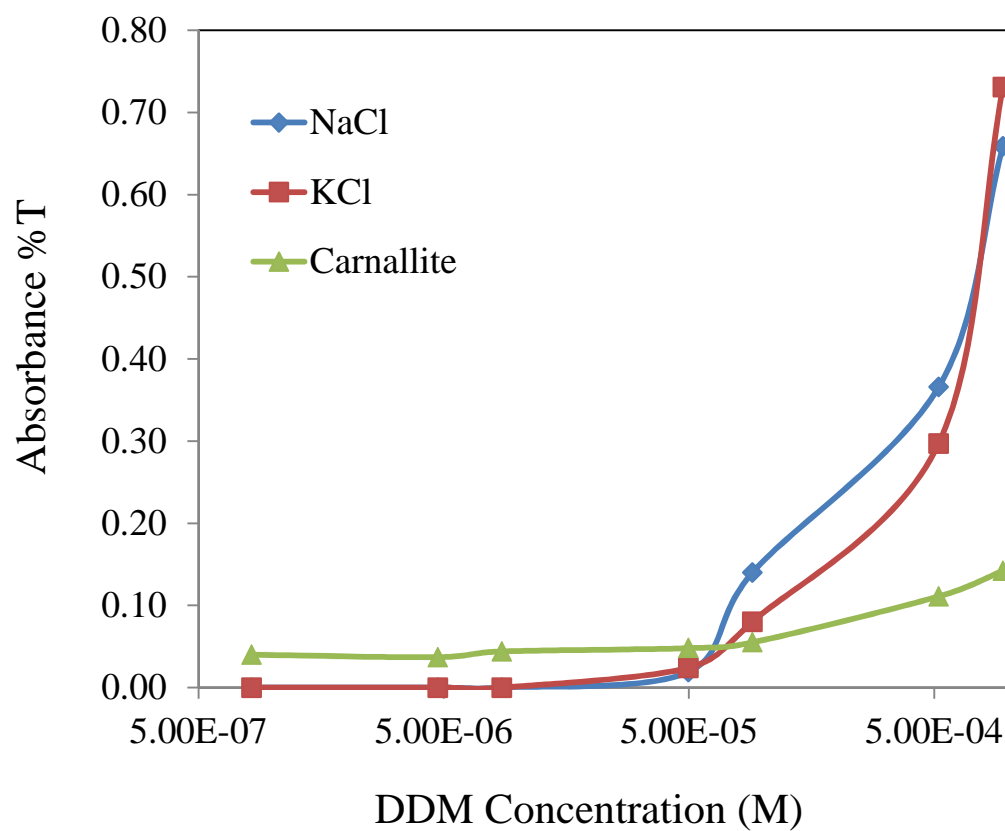


Figure 3.5 The turbidity absorbance of DDM in saturated solutions of KCl, NaCl and carnallite.

lower levels of turbidity and may indicate that the DDM precipitates form large aggregates and exhibit a lower degree of dispersion. The results suggest that the DDM colloid may precipitate at the NaCl or KCl particle surfaces, and in this way flotation is facilitated. At  $1 \times 10^{-4}$  M DDM, almost 90% of NaCl has been floated.

### 3.3.3 Zeta Potential of DDM Collector Colloid

Usually DDM is considered as a cationic collector of the form  $\text{DDMH}^+$  in solution. In this study a DDM hydrochloride was used. Precipitation of the  $\text{DDMHCl(s)}$  colloid is expected for which the zeta potential and its sensitivity to pH have been established as shown in Figure 3.6. The results indicate that, when the solution pH is lower than pH 6, the DDM colloid has a positive surface charge, while DDM has a negative charge at pH values higher than 6. The results indicate that the DDM precipitate has an isoelectric point at about pH 6. In brine solutions, due to high ionic strength, the electrical double layer is compressed, and direct measurement of zeta potential is difficult. As discussed in Chapter 1, the sylvite mineral has a negative charge, and halite has a positive charge. Based on flotation results and FTIR results reported in Chapter 2, adsorption of the DDM colloid does not seem to be influenced by particle surface charge.

## 3.4 Summary

Surface-tension measurements for DDM in NaCl- and KCl-saturated solutions were performed. A surface-tension plateau was reached at approximately  $2 \times 10^{-5}$  M DDM, which appears to correspond to the concentration for precipitation of the DDM colloid. Turbidity measurements for DDM in NaCl- or KCl-saturated solutions indicated that at  $5 \times 10^{-6}$  M DDM the turbidity increased, indicating precipitation of the collector colloid. Therefore the precipitation concentration for DDM was determined to be

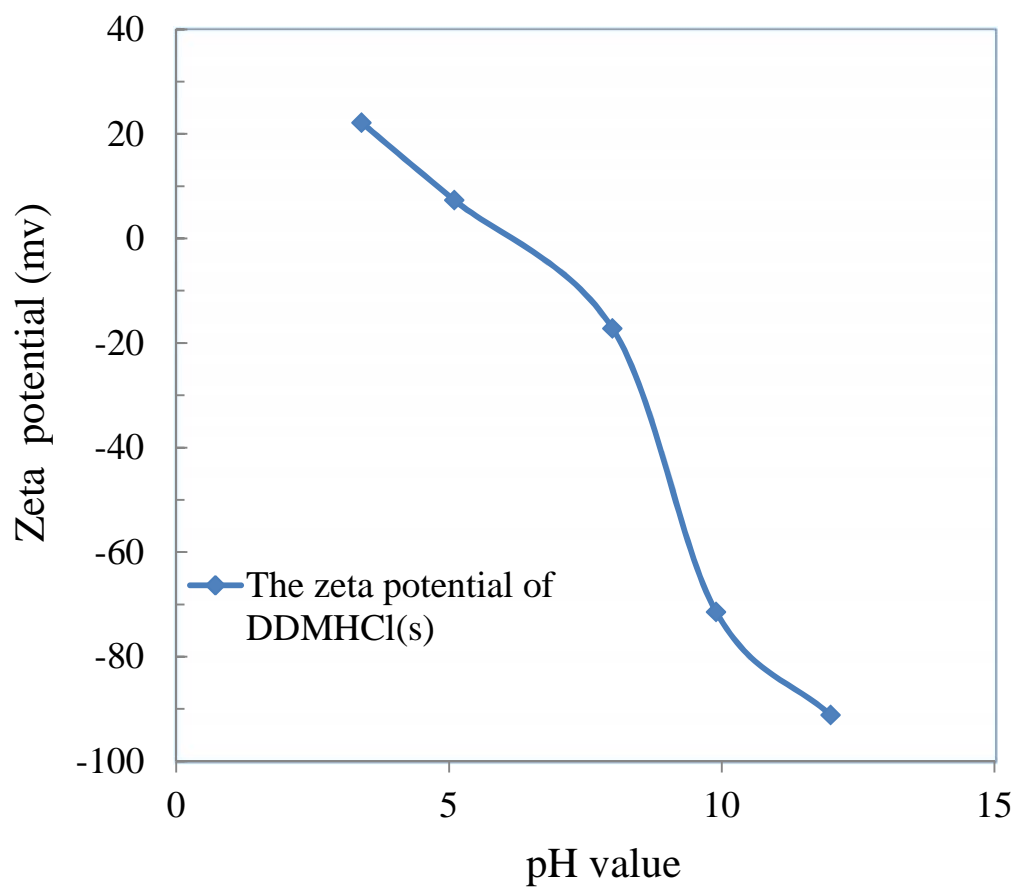


Figure 3.6 Zeta potential of DDM colloid in DI-water as a function of pH.

between  $1.8 \times 10^{-5}$  M and  $2 \times 10^{-5}$  M for NaCl and KCl brines. In the case of carnallite, the precipitation concentration is about  $1 \times 10^{-4}$  M of DDM, much higher than in NaCl- or KCl-saturated solution. It is possible that, during flotation, DDM first precipitates at the surfaces of NaCl and KCl particles. When the DDM concentration reaches  $1 \times 10^{-4}$  M DDM, the precipitation concentration in carnallite brine, almost 90 to 95% of the NaCl and KCl particles have been floated. It seems that collector colloid precipitation at the surface of salts particle may play a significant role in the flotation of halite and sylvite from carnallite.

## CHAPTER 4

### WETTING CHARACTERISTICS OF HALITE, SYLVITE AND CARNALLITE SURFACES

#### 4.1 Introduction

Contact angle measurements describe the wetting characteristics of surfaces and can be accomplished using such methods as the sessile drop or captive bubble methods. The contact angle is the angle between the liquid/vapor interface and the solid surface measured through the liquid phase, as shown in Figure 4.1. The concept of a contact angle was first described quantitatively by Young in his 1805 essay on the cohesion of fluids. The relationship between contact angle and interfacial tensions is described by the Young-Laplace equation,

$$\gamma_{sv} = \gamma_{sl} + \gamma_{lv} \cos \theta \quad (\text{Young-Laplace equation})$$

where  $\gamma_{sv}$  is the solid/vapor surface free energy,  $\gamma_{sl}$  is the solid/liquid interface free energy,  $\gamma_{lv}$  is the liquid/vapor surface tension, and  $\theta$  is the wetting contact angle. According to the equilibrium state, the contact angle is established by a balance of forces in the horizontal direction; the smaller the contact angle, the better the wetting characteristics and the more hydrophilic the surface. In this way the wetting characteristics are frequently described from contact-angle measurements.

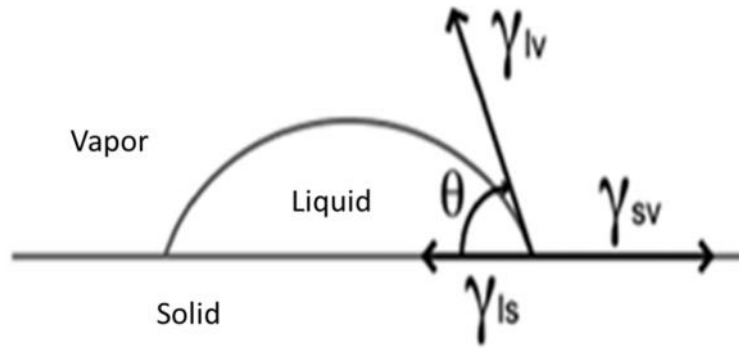


Figure 4.1 Schematic of a sessile-drop contact angle.

It can be seen that the adsorption of collector (surfactant) will reduce the interface tension and thus will change the contact angle or surface wettability. Change in the wetting characteristics can be used to identify the adsorption of collector at a solid surface. In other words, for DDM collector adsorption at a NaCl or KCl surface, the contact angle will increase and a hydrophobic surface will be created. Thus the particle will attach to an air bubble and will float during flotation. If there is no adsorption of DDM collector, then the contact angle will be close to zero for naturally hydrophilic surfaces. Under these circumstances, flotation will not occur.

In this chapter, captive-bubble contact-angle measurements to investigate the wetting characteristic at halite (NaCl), sylvite (KCl), and carnallite ( $\text{KMgCl}_3 \cdot 6\text{H}_2\text{O}$ ) surfaces with different concentrations of DDM are described.

Bubble attachment-time measurement is another way to describe the wetting characteristics of mineral surfaces. Attachment time is defined as the time needed for attachment of particles to an air bubble when they are in proximity. The bubble/particle attachment interactions are determined by the colloid and surface chemistry aspects of both the particle and the air bubble, which are established by adsorption of surfactants at

the interface. Bubble attachment-time measurements provide a useful methodology to study some significant flotation variables, such as pH, particle size, reagent type and concentration, electrolyte ionic strength, bubble charge, and temperature. The measurement takes into account both hydrodynamics and the surface chemistry of flotation. In this study the bubble attachment time was measured as function of collector concentration.

## **4.2 Material and Experimental Methods**

### **4.2.1 Contact-Angle Measurements**

Contact angles were measured with a NRL goniometer using the captive-bubble technique. For each measurement, a 50-mm  $\times$  25-mm  $\times$  6-mm NaCl or KCl crystal substrate was first dry polished with 600 grit paper. After removing residual particles with compressed nitrogen gas, the crystal plate was cleaned in plasma for 5 min to obtain a fresh crystal surface. The reagent, 4-dodecyl morpholine-4-hydrochloride with a purity of 99%, was purchased from Sigma Aldrich. All reagents were used without any further purification. Deionized water (18 M  $\Omega$ ) was used in all the experiments. All glassware was soaked in chromic acid, rinsed with purified water and dried prior to use.

In the captive-bubble experiments, the NaCl or KCl crystal plate was immersed in the solution and the system was equilibrated for 8 min. Then an air bubble was introduced with a micro-syringe through a U-shaped needle underneath the substrate surface. After air-bubble attachment, the contact angle on both sides of the bubble was measured at 5-min intervals at 24°C.

Preparation of the saturated salt solution is very important. Because solubility of the salt is highly dependent on temperature, a small change in temperature will cause fine crystals to dissolve or crystallize from the solution. In either case, measurement errors



will be significantly increased. The preparation of saturated brine and the experiments were done at room temperature. In the case of NaCl and KCl a sufficient amount of each salt was dissolved in Millipore water and stirred overnight to achieve saturation.

#### 4.2.2 Bubble Attachment Time

An MCT-100 Electronic Induction Timer (Figure 4.2) was used to measure the bubble attachment time at the surfaces of NaCl, KCl, and  $\text{KMgCl}_3 \cdot 6\text{H}_2\text{O}$  salt particles with DDM as collector. Particle size has a significant influence on bubble attachment time (Ye et al., 1989), which decreases with a decrease in particle size. In this regard, salt particles of  $80 \times 100$  mesh fraction were prepared for this experiment. The measurement procedure is as described below.

First, the desired amount of collector was added to saturated brines of the selected salts. Then, 1 g of salt sample ( $80 \times 100$  mesh) was added to the saturated solution with collectors, and the suspension was stirred for 15 min to establish equilibrium in the

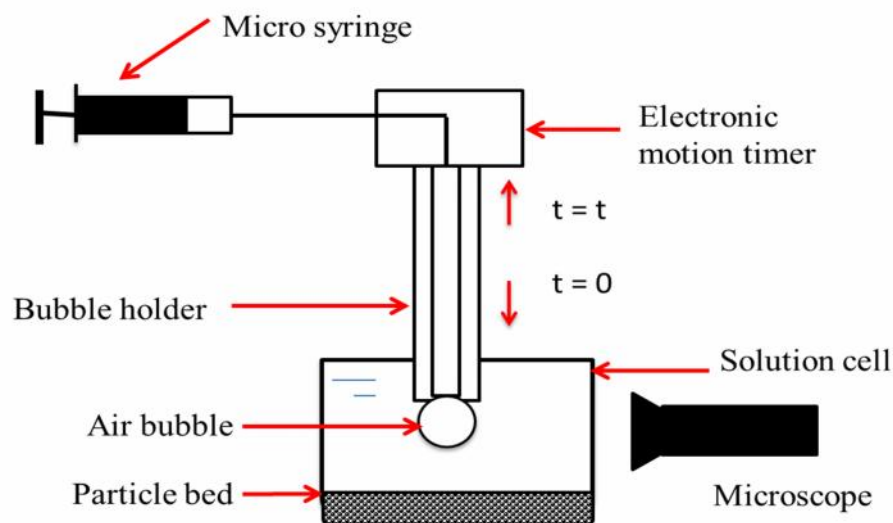


Figure 4.2 Schematic of MCT-100 Electronic Induction Timer.

induction timer cell. The mixture was settled for another 5 min to form a stable particle bed before measurement.

All measurements were performed at room temperature. In each test, an air bubble of 3 mm diameter was generated with a micro syringe. Then the distance between the air bubble and the particle bed was adjusted by the micro-scale of the microscope. The bubble was brought down to contact the surface of the particle bed at a specified contact time automatically controlled by the instrument.

After that, whether particles attached to the air bubble was determined by visual observation through the microscope. Any particle attached to the air bubble surface was defined as an attachment event (Figure 4.3). A set of 10 measurements was performed at different places on the particle bed and the observations were recorded. The number of observations with attachment was divided by the total number of observations and recorded. Bubble attachment time is defined as the time at which 50% of contacts resulted in successful attachment.

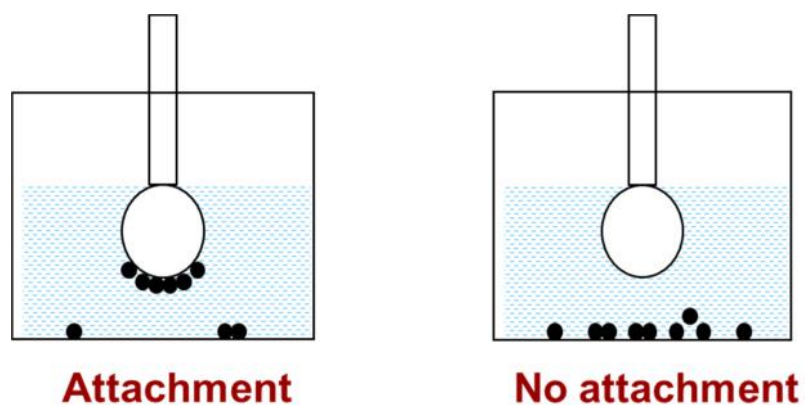


Figure 4.3 Attachment event.

### 4.3 Results and Discussion

#### 4.3.1 Contact-Angle Measurements

In these experiments, the influence of DDM addition on contact angles at the NaCl and KCl salt surfaces was studied, and the results are shown in Figures 4.4 and 4.5. Figure 4.4 shows clearly that the contact angle at an NaCl surface increased with an increase in DDM concentration. It can be seen that the contact angle started increasing at the concentration of  $3 \times 10^{-6}$  M DDM. When the concentration increased to  $1 \times 10^{-5}$  M, the contact angle at the NaCl surface was about 44 degrees and then remained constant.

As seen from the contact-angle data for KCl in Figure 3.5, at low DDM concentrations the contact-angle change was not significant, but when the concentration was higher than  $2 \times 10^{-5}$  M the contact angle increased significantly. At a concentration of  $5 \times 10^{-5}$  M, the contact angle reached 35 to 40 degrees. Above this concentration the contact angle remained constant. It appears that, after conditioning with DDM, NaCl gives a higher final contact angle than that observed for KCl.

These results are in good agreement with the results from microflotation and imply that NaCl flotation with DDM is more efficient than KCl flotation with DDM. At a concentration of  $2 \times 10^{-5}$  M of DDM, a flotation recovery of 94% can be achieved for NaCl, while 80% recovery was obtained for KCl. Contact-angle measurements indicate that DDM adsorbed at both the NaCl and KCl surfaces and created a hydrophobic surface state. Therefore either NaCl and KCl can be floated from a saturated solution using DDM as a collector.

Shown in Figure 4.6 are the results from contact-angle measurements in DDA solution. It can be seen that, when DDA concentration was higher than  $5 \times 10^{-5}$  M at

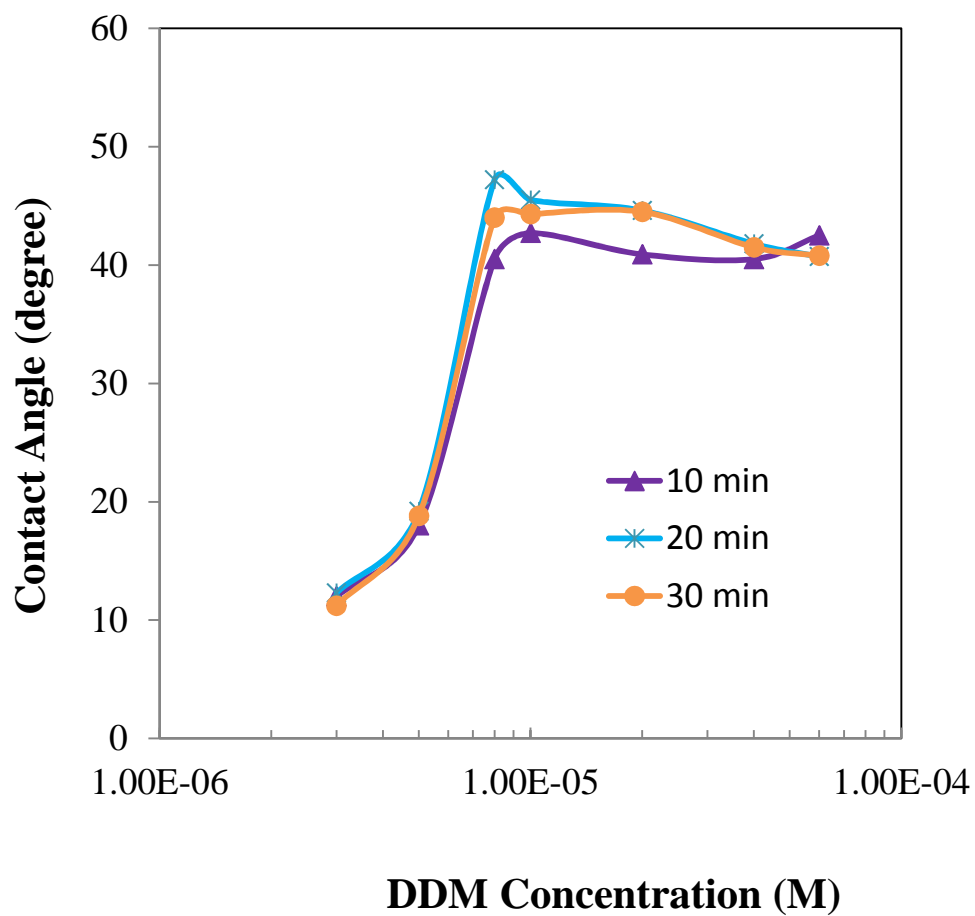


Figure 4.4 Contact angle at an NaCl surface in DDM solution as a function of DDM concentration.

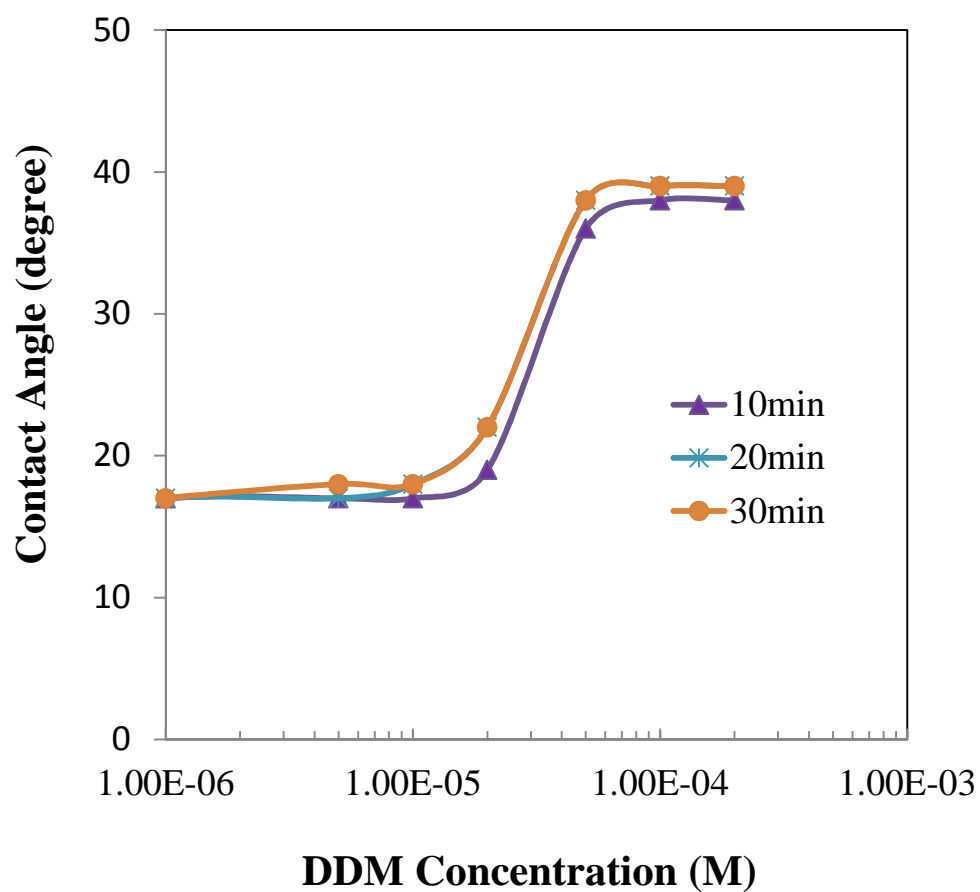


Figure 4.5 Contact angle at a KCl surface in DDM solution as a function of DDM concentration.

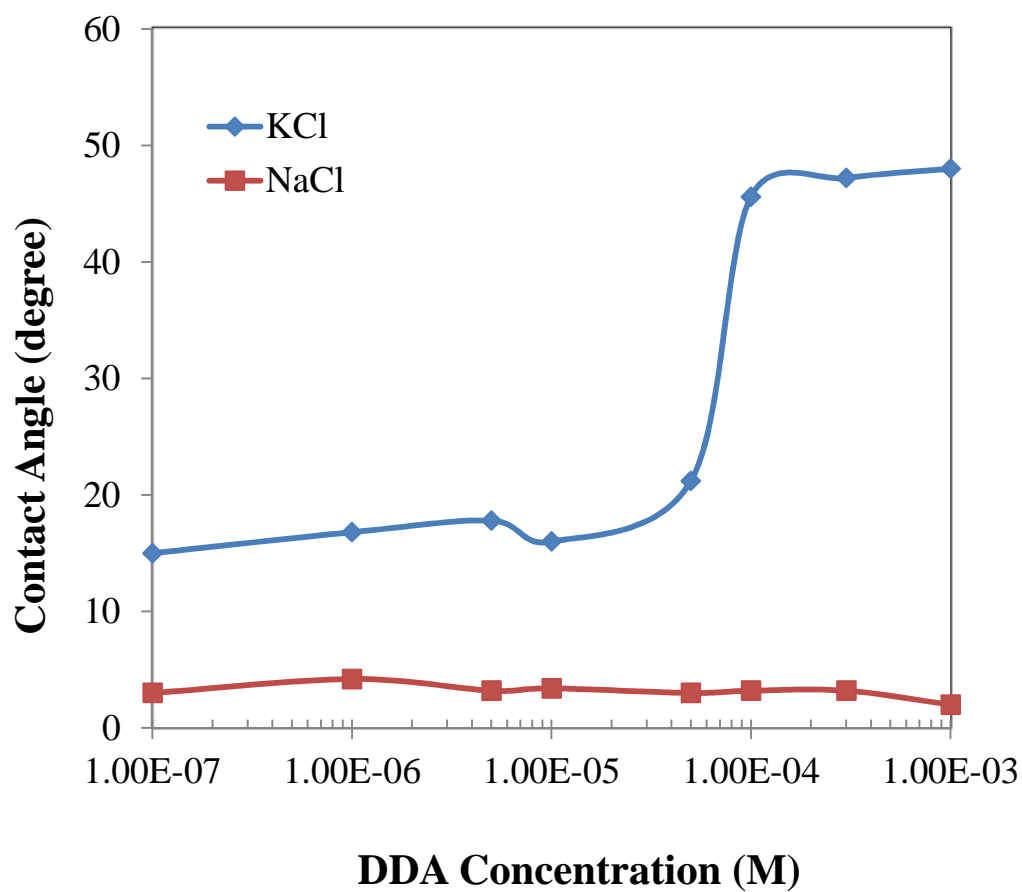


Figure 4.6 Contact angle at NaCl and KCl surfaces in DDA solution as a function of DDA concentration.

the KCl surface, the contact angle significantly increased, but the contact angle at the NaCl surface was almost unchanged. These results indicated that the amine adsorbed selectively at the KCl surface but not at the NaCl surface. Therefore, for the amine flotation system, only KCl can be floated using dodecyl amine as collector.

#### 4.3.2 Bubble Attachment Time

Figures 4.7, 4.8, and 4.9 show the results from bubble-attachment experiments. The results clearly show that the attachment time for NaCl particles decreased when the DDM concentration increased. When the DDM concentration increased to  $5 \times 10^{-6}$  M from  $1 \times 10^{-6}$  M, the attachment time decreased significantly from 650 ms to 40 ms. This concentration is close to that at which the contact angle started to change significantly. The microflotation results indicated that, when the DDM concentration reached  $5 \times 10^{-6}$  M, flotation occurred, and, when the concentration increased to  $1 \times 10^{-5}$  M, 41% NaCl recovery was achieved.

In the case of KCl particles, the same trend (Figure 4.7) was observed. When the concentration of DDM increased from  $1 \times 10^{-6}$  M to  $6 \times 10^{-6}$  M, the attachment time reduced from 300 ms to 30 ms. For carnallite, attachment was not observed, as evidenced by the data presented in Figure 4.9.

The results from bubble-attachment experiments indicate that DDM adsorbed selectively at the NaCl and KCl surface but not at the carnallite surface. All results from microflotation, contact-angle, and bubble-attachment experiments show a critical concentration, about  $5 \times 10^{-6}$  M of DDM. At this concentration the bubble attachment time was about 30 ms. The results from microflotation indicate that a DDM solution at  $5 \times 10^{-6}$  M DDM was required for flotation to be initiated, as shown in Figure 2.3.

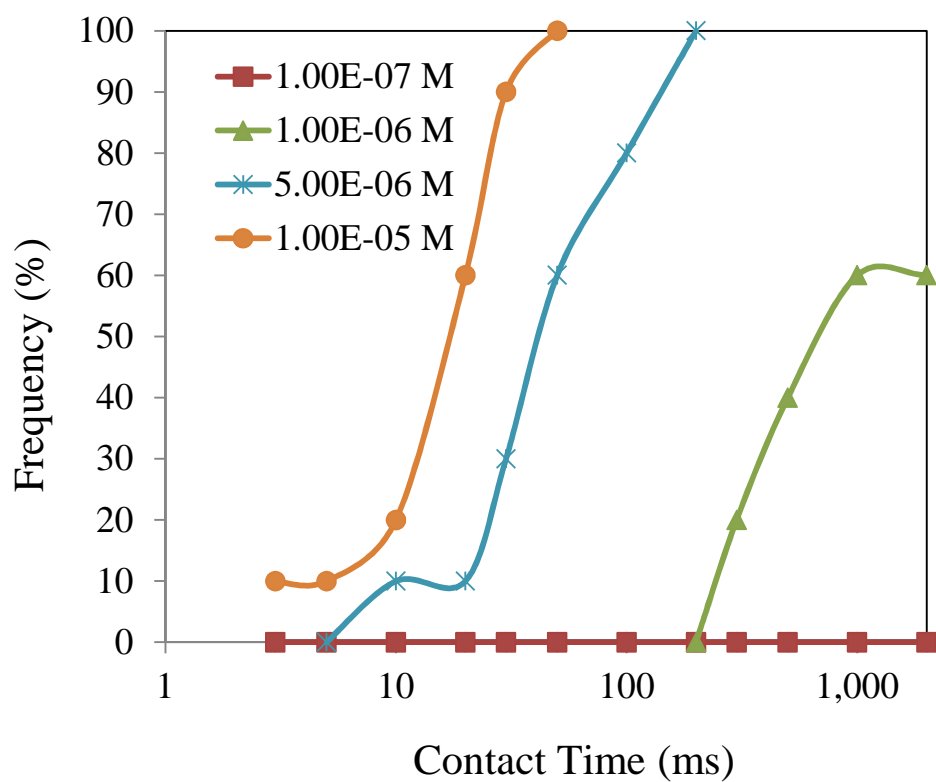


Figure 4.7 Bubble attachment-time results for NaCl in DDM solutions of different concentrations.



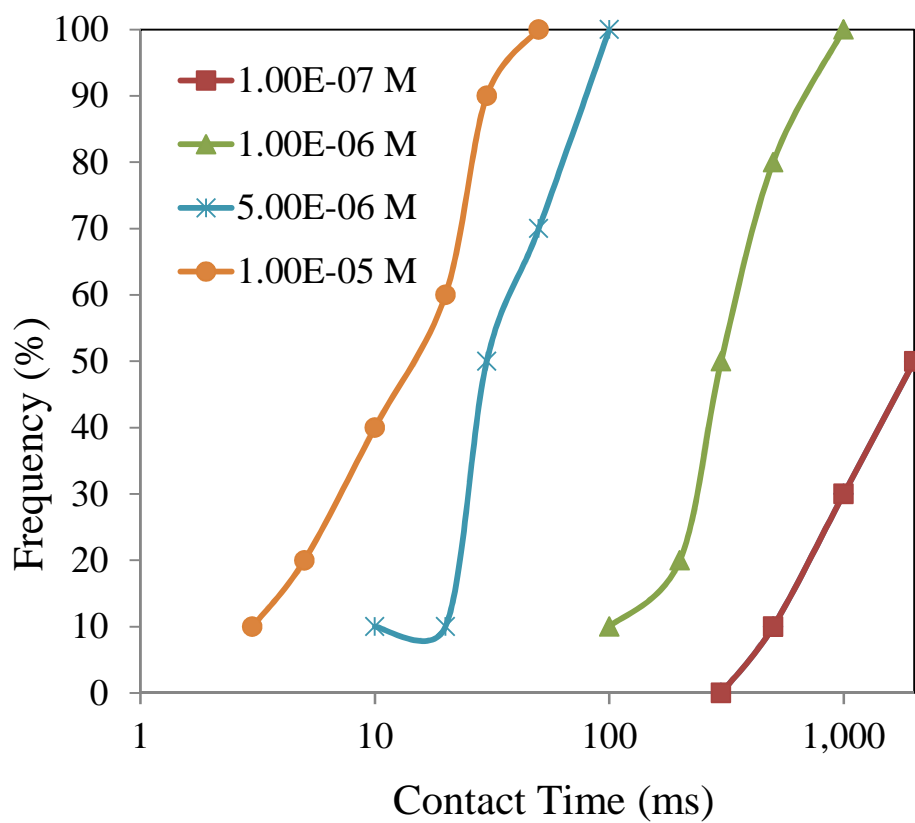


Figure 4.8 Bubble attachment-time results for KCl in DDM solutions of different concentrations.

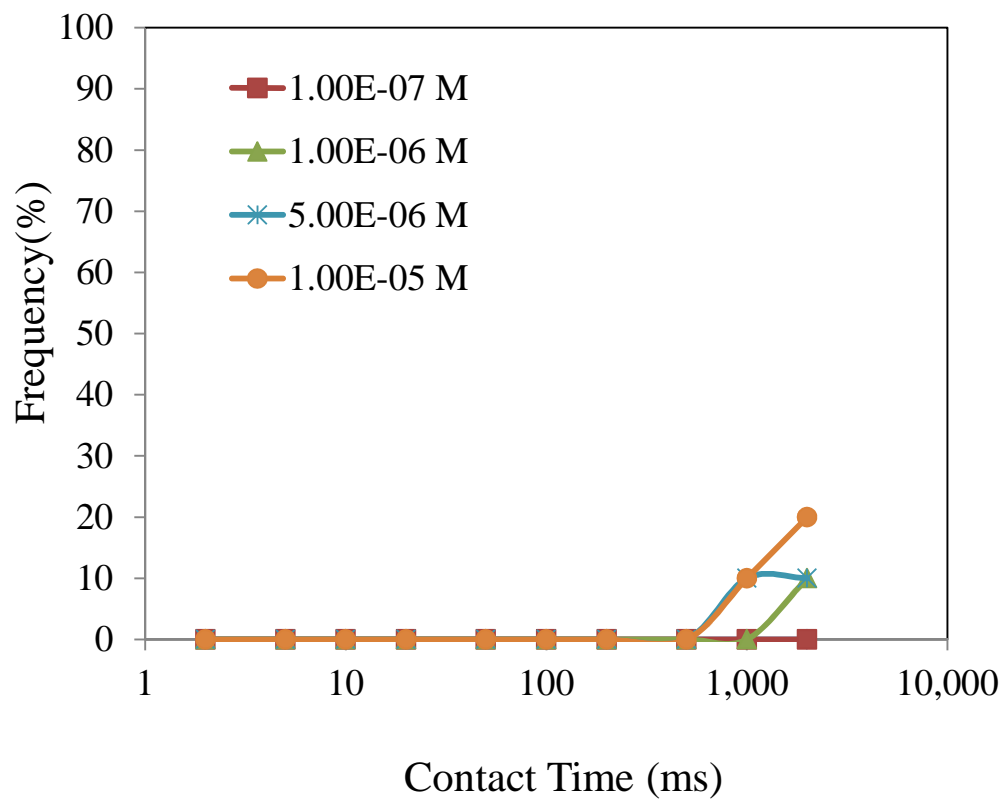


Figure 4.9 Bubble attachment-time results for carnallite in DDM solutions of different concentrations.

#### 4.4 Summary

The results from contact-angle measurements for KCl and NaCl in saturated solutions with DDA indicate that DDA was selectively adsorbed at the KCl surface and the contact angle increased with DDA concentration, while, for NaCl, the contact angle was only a few degrees and did not change with an increase in DDA concentration. The results indicate that only KCl can be floated using dodecyl amine as collector.

Contact-angle measurements for NaCl and KCl in saturated solutions with DDM at different concentrations showed that the contact angle for both NaCl and KCl increased with an increase in DDM concentration. The results indicate that DDM is adsorbed at both the NaCl and the KCl surfaces and also suggest that either NaCl and KCl can be floated using DDM as collector.

Bubble attachment-time measurements for KCl and NaCl indicate that the attachment time reduced when the DDM concentration increased. At a concentration of  $5 \times 10^{-6}$  M DDM, the attachment time was reduced to about 30 to 40 ms. This is the same concentration at which flotation started.

Results from contact-angle measurements and bubble attachment-time experiments indicate that, for both NaCl and KCl, a significant surface-state change occurs at a certain DDM concentration. This critical concentration is about  $2 \times 10^{-5}$  M DDM and is in the range of concentration needed for flotation, as discussed in Chapter 3. This concentration may correspond to the DDM precipitation concentration at the surface of NaCl and KCl particles.

Because of the difficulty in obtaining a carnallite substrate, contact-angle measurements were not done for carnallite. Bubble attachment-time measurements showed that attachment was not successful for the DDM concentration range studied.

# **CHAPTER 5**

## **MOLECULAR DYNAMIC SIMULATIONS OF INTERFACIAL WATER AT SYLVITE, HALITE, AND CARNALLITE SURFACES**

### **5.1 Introduction**

Previous studies of interfacial water structure at salt surfaces indicated that interfacial water may play an important role regarding collector adsorption. As mentioned in Chapter 1, the alkali halides are generally categorized as either water structure makers or water structure breakers. Structure-breaking salts such as KCl can be floated with either anionic (SDS) and cationic (amine) surfactants. On the other hand, it appears that no collector adsorption occurs at structure-making salt surfaces such as NaCl, and these salts cannot be floated, as indicated by the microflotation results presented in Chapter 2.

Despite the success of the structure-making/breaking concept in explaining the different flotation behavior of NaCl and KCl, there are still issues that require further attention. For example, microflotation results using dodecyl morpholine (DDM) as collector indicated that both NaCl and KCl can be floated using DDM as collector but that carnallite cannot be floated. In the morpholine flotation system, it seems that morpholine collector adsorbs at the surface of the structure-making salt NaCl, and in fact this was verified by FTIR analysis, as described in Chapter 2. In this chapter, based on

molecular dynamic simulations (MDS) done by Jin (2012), more information and understanding regarding interfacial water structure and its dynamics at NaCl, KCl and carnallite surfaces are provided. It should be noted that a simplified crystal force field was used for the salt, and a more accurate force field such as used by Du and Miller (2007) will be needed in further research.

## 5.2 Molecular Dynamics Simulation

The MD simulation package Amber 9 was used for the analysis of interfacial water structure at the NaCl, KCl, and carnallite surfaces. The simple point charge (SPC) water model (Berensen, 1981) was used to describe the interaction parameters for water molecules. The pair potential force field used in the simulations is given as a combination of the Lennard-Jones and the Coulomb electrostatic interactions, and can be expressed as:

$$\phi(r_{ij}) = 4\epsilon_{ij} \left[ \left( \frac{\sigma_{ij}}{r_{ij}} \right)^{12} - \left( \frac{\sigma_{ij}}{r_{ij}} \right)^6 \right] + \frac{q_i q_j}{r_{ij}}$$

where  $r_{ij}$  is the distance between particles  $i$  and  $j$ ,  $\sigma$  and  $\epsilon$  are the size parameter and energy parameter, respectively, and  $q_i$  is the charge of the  $i^{\text{th}}$  atom (or ion).

A cubic cell containing the salt crystal surface and water molecules was constructed with periodic boundary conditions. The initial configurations of the salts were constructed using lattice parameters provided by the American Mineralogist Crystal Structure Database (Gruner, 1934; Perdikatsis and Burzlaff, 1981). The size of the simulation cells as well as the number of alkali halide ions and the number of water molecules in each simulation cell are summarized in Table 5.1. The water density distribution and water residence time were extracted from Amber MD simulation for

Table 5.1 Salt Parameters for Molecular Dynamics Simulations

Parameter	Salt								
	Halite			Sylvite			Carnallite		
	Type	Re/2 ( )	(kcal/mol)	Type	Re/2 ( )	(kcal/mol)	Type	Re/2 ( )	(kcal/mol)
Force field	-	-	-	K	1.8694	0.1	K	1.8694	0.1
	N	1.4497	0.1	-	-	-	Mg	2.9548	0
	Cl	2.4699	0.1	Cl	2.4699	0.1	Cl	2.4699	0.1
	Type	Number		Type	Number		Type	Number	
Periodic box	-	-		K	500		K	144	
	Na	500		-	-		Mg	144	
	Cl	500		Cl	500		Cl	432	
	Water	1034		Water	1096		Structure water	864	
							Solvate water	2600	
Box size	30×30×70	( )		30×30×70	( )		50×50×60	( )	

interfacial water structure and water stability analysis at the salt surfaces. An initial simulation of alkali halide salts in saturated brines was performed for 1 ns ( $10^6$  steps each of 1 fs) to achieve an equilibrated ion and water distribution.

Figures 5.1 and 5.2 are MDS close-up snapshots of water molecules near NaCl, KCl and carnallite surfaces, taken at the equilibrium state (1 ns). From the MDS snapshot of water molecules near the carnallite surface in Figure 5.2, it can be seen that water molecules strongly interact with the surface  $\text{Cl}^-$  ions, unlike the interactions with NaCl and KCl shown in Figure 5.1.

### 5.3 Water Density Distributions at NaCl, KCl, and Carnallite Surfaces

The relative ion density distributions by number along the surface normal, obtained from MD simulation, is shown in Figures 5.3, 5.4, and 5.5. The orientation of

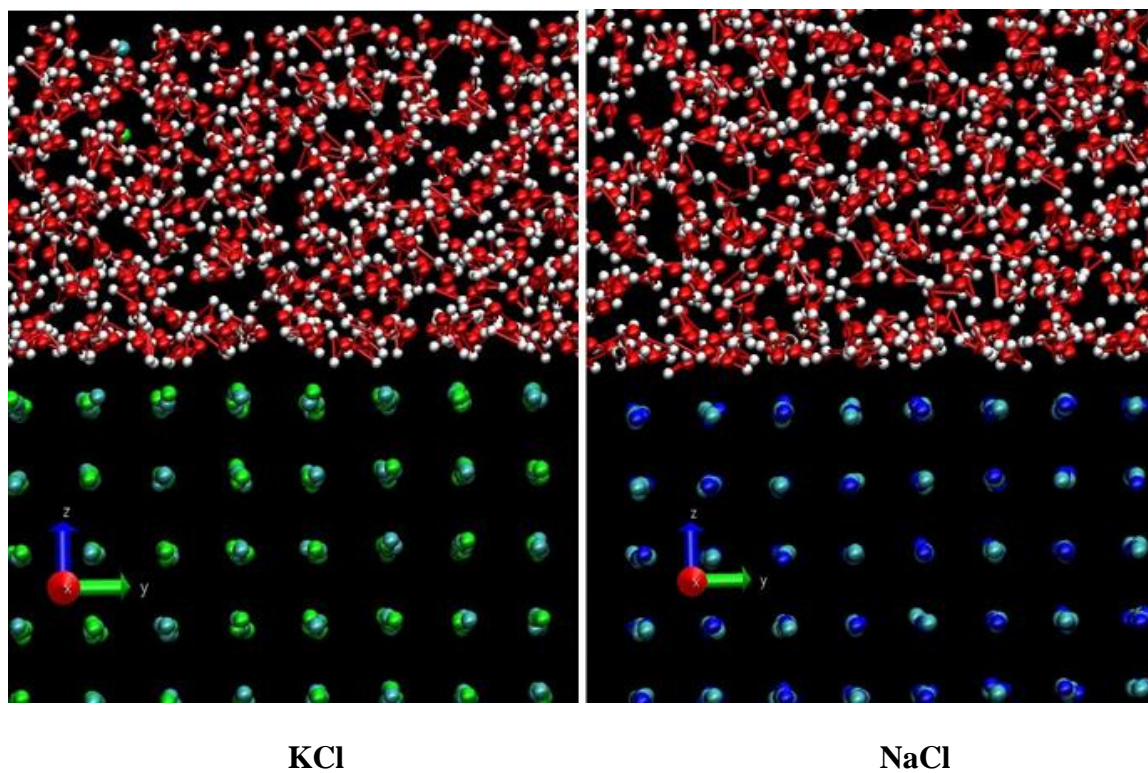


Figure 5.1 Close-up MDS snapshots of water molecules near KCl and NaCl surfaces, taken at the equilibrium state (1 ns).

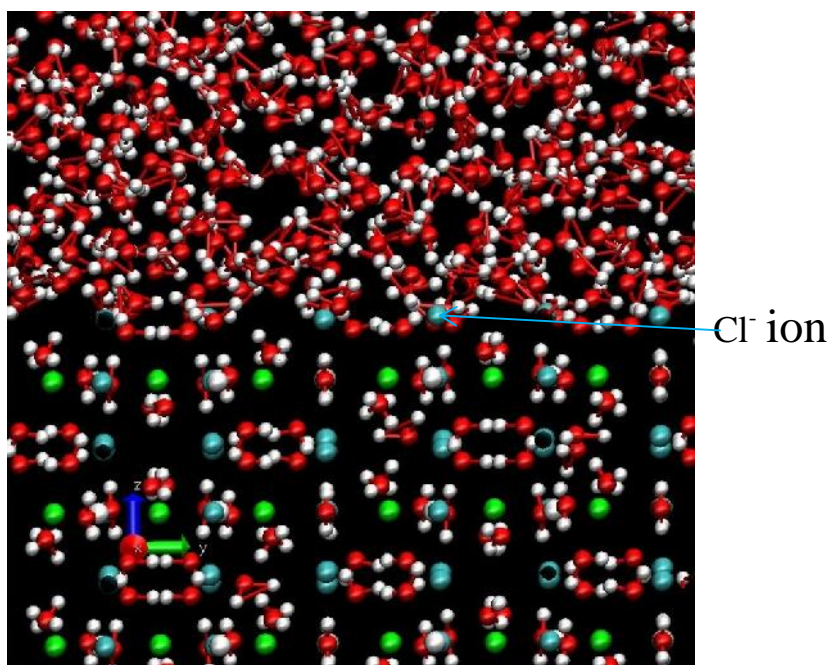


Figure 5.2 Close-up MDS snapshot of water molecules near a carnallite surface, taken at the equilibrium state (1 ns).



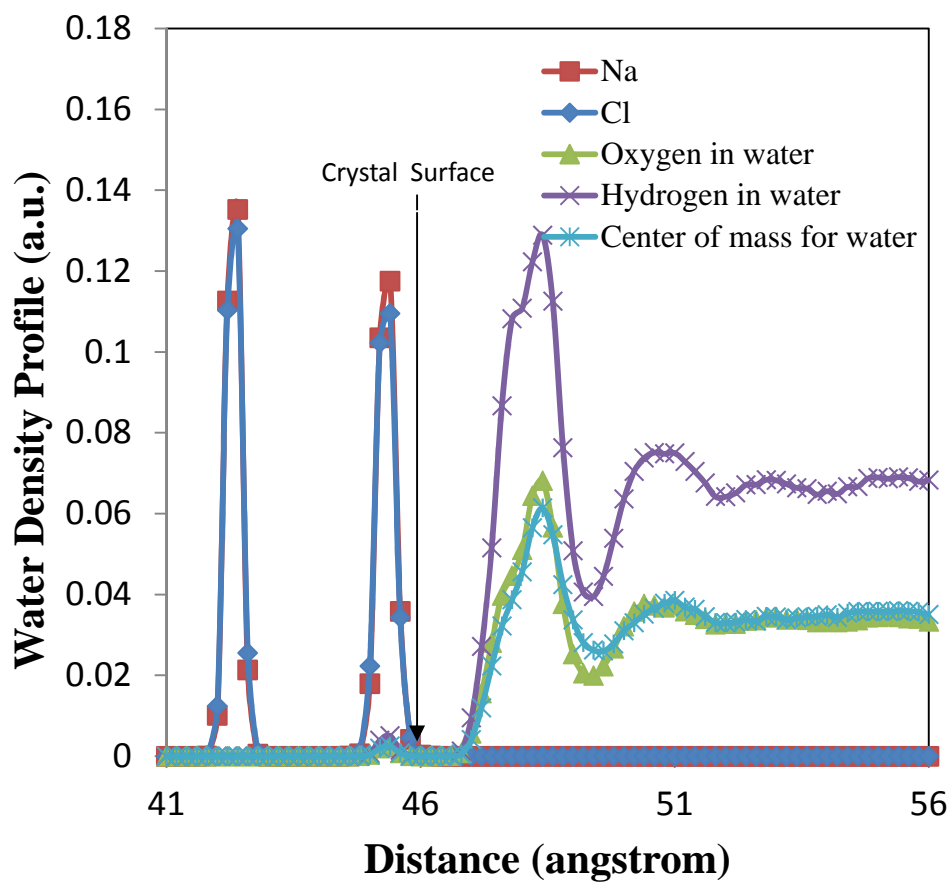


Figure 5.3 Water density profile at the water/NaCl interface.

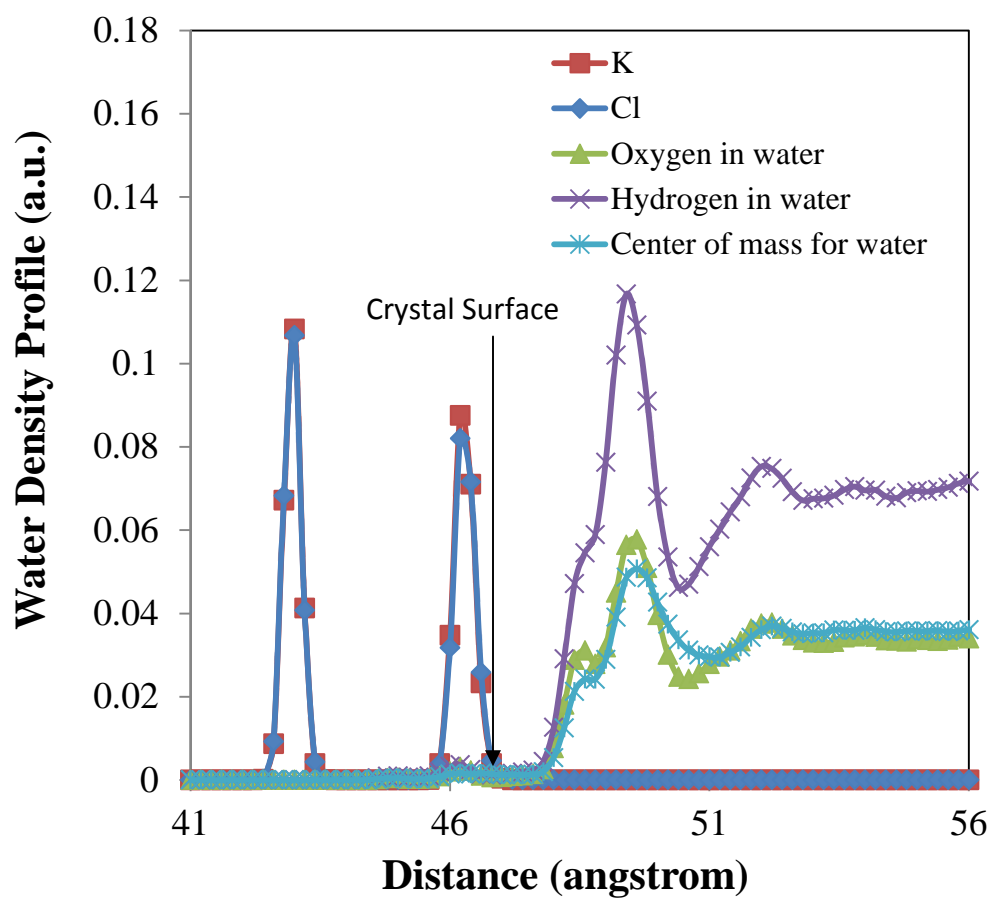


Figure 5.4 Water density profile at the water/KCl interface.

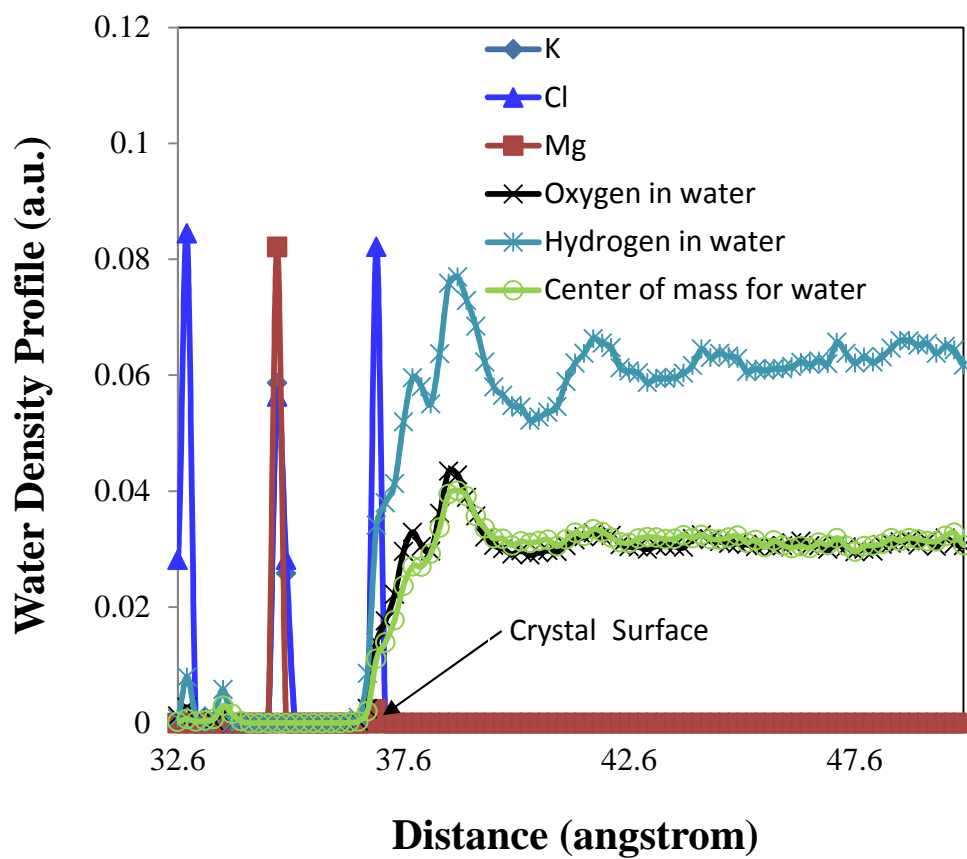


Figure 5.5 Water density profile at the water/carnallite interface.

water molecules at the salt surface can be studied by analyzing the position of the oxygen atom relative to the position of the hydrogen atoms in the water molecules. A water molecule's oxygen atoms are away from the NaCl crystal surface, while the water's hydrogen atoms are closer to the surface. In this case there is a parallel hydrogen/oxygen configuration of the interfacial water structure. For KCl, the interfacial water has a hydrogen/oxygen/hydrogen configuration for interfacial water due to the increase in cation size.

In the case of the carnallite surface the water density profile (Figure 5.5) shows that the water molecules are overlapped with the surface  $\text{Cl}^-$  ions. Again this indicates that the water molecules interact strongly with surface  $\text{Cl}^-$  ions. The MDS results imply that the carnallite surface is completely and strongly hydrated.

#### **5.4 Water Residence Times at Salt Surfaces**

Residence time was analyzed to understand how tightly water molecules are bonded to the surface and how long a water molecule will stay in each water layer. As shown in Figure 5.6, the water residence time at the NaCl surface is about 30 ps, which is longer than that at the KCl surface, 20 ps. This means that interfacial water is more stable at the NaCl surface than at the KCl surface. However, when compared with carnallite's, NaCl's and KCl's water residence times of 20 or 30 ps are very short, because the water residence time at the carnallite surface is longer than the simulation time (1000 ps) for the water/carnallite system. This may be the major reason that carnallite cannot be floated using DDM or amine collectors for that matter. The results from residence-time calculations are summarized in Table 5.2.

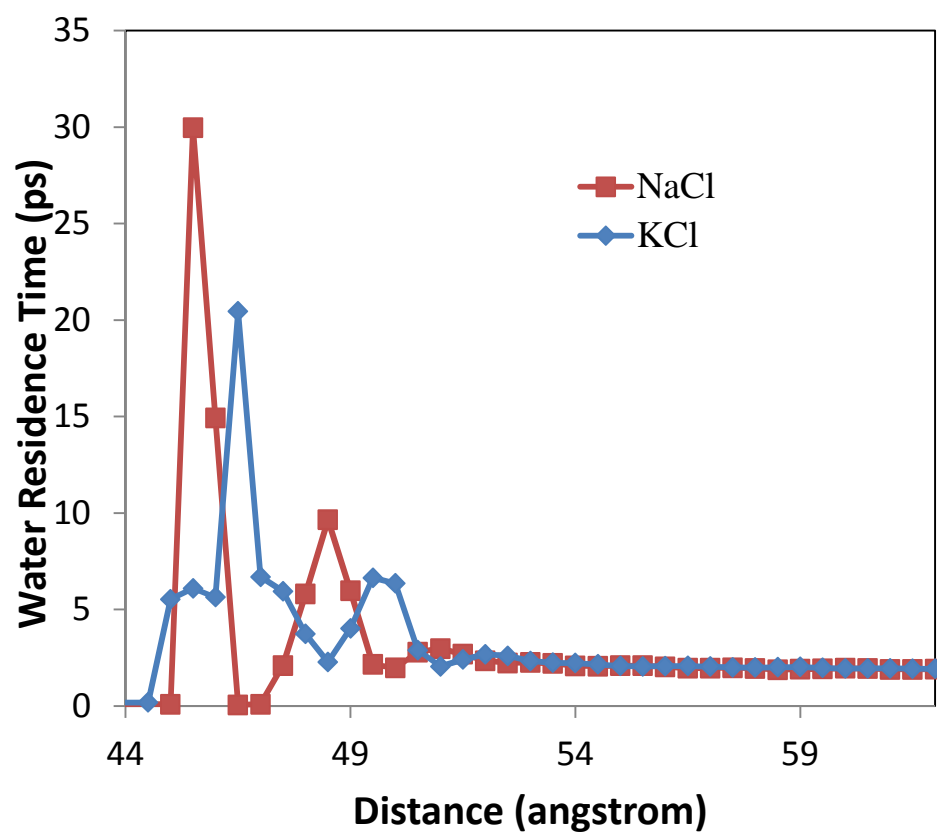


Figure 5.6 Water residence times at the water/NaCl and water/KCl interfaces.

Table 5.2 Water Residence Times at Water/Salt Interfaces

Interface	Water Residence Time (ps)
Water/NaCl	30
Water/KCl	20
Water/Carnallite	Longer than simulation time (1000 ps)

### 5.5 Summary

Water residence time at the NaCl surface is about 30 ps, which is longer than that at the KCl surface, 20 ps. This means that interfacial water is more stable at the NaCl surface than at the KCl surface. In the case of carnallite, the surface is completely hydrated, and the residence time is exceedingly long due to the strong surface hydration. Therefore, the collector molecules or the collector colloid cannot replace interfacial water molecules at the surface of carnallite, and the particles remain in a hydrophilic state during flotation with DDM. On the other hand, water is not stable at the surfaces of NaCl and KCl due to the shorter water residence time; thus a collector molecule can replace a water molecule and be adsorbed at the surfaces of NaCl or KCl.

## CHAPTER 6

### SUMMARY AND CONCLUSIONS

Microflotation experiments were carried out to study the flotation response for KCl, NaCl, and carnallite using morpholine as a collector. The flotation results indicate that either NaCl or KCl can be floated well using morpholine collector, but carnallite cannot be floated. Examination of flotation products using FTIR shows that morpholine selectively adsorbed at the surfaces of NaCl and KCl particles. There is no indication of morpholine adsorption at the surface of carnallite. The results also show that, when the morpholine concentration reached  $2 \times 10^{-6}$  M, flotation of NaCl and KCl started. When the morpholine concentration increased to  $1 \times 10^{-4}$  M, a flotation recovery of 90% for NaCl could be achieved.

The wetting characteristics of NaCl, KCl, and carnallite were studied by means of contact-angle measurements and bubble-attachment experiments. The results from contact-angle measurements as a function of morpholine concentration indicate that, when the concentration of morpholine increased to  $2 \times 10^{-6}$ , an increase in contact angle occurred at the surfaces of NaCl and KCl. A maximum contact angle of 44 degrees at the NaCl surface could be reached at  $1 \times 10^{-5}$  M morpholine concentration. In the case of the KCl surface, the maximum contact angle was about 35 degrees at a morpholine concentration of  $5 \times 10^{-5}$  M. The results from bubble-attachment experiments show a critical concentration. When the concentration of morpholine increased to  $5 \times 10^{-6}$  M from  $1 \times$

$10^{-6}$  M, the bubble attachment time was significantly reduced. For NaCl particles, the bubble attachment time reduced to 40 ms from 650 ms. The bubble attachment time on KCl particles reduced to 30 ms from 300 ms. The contact angle onto carnallite did not change in the concentration range studied. No bubble-attachment event happened.

In order to further evaluate the morpholine concentration effect, surface-tension and turbidity measurements as functions of morpholine concentration in salt-saturated solutions were carried out. Surface-tension measurements indicated that there is a minimum transition concentration around  $2 \times 10^{-5}$  M in NaCl- or KCl-saturated solution. After this concentration the surface tension remained almost constant. At a concentration of  $5 \times 10^{-6}$  M, an increase in turbidity could be observed. This concentration may correspond to morpholine precipitation concentration.

According to all the experimental data for flotation, contact angle, bubble attachment, surface tension, and turbidity, it is reasonable to consider the morpholine precipitation concentration in NaCl- or KCl-saturated solution to be in the  $5 \times 10^{-6}$  to  $1 \times 10^{-5}$  M range. If this is true the adsorption of the morpholine collector may be related to morpholine precipitation at the NaCl and KCl surfaces. In a carnallite-saturated solution, the minimum transition concentration was about  $1 \times 10^{-4}$  M morpholine. This implies that morpholine precipitation concentration in a carnallite-saturated solution was much higher than in NaCl- or KCl-saturated solutions. In this regard, morpholine may first selectively precipitate at the surface of NaCl or KCl particles and create a hydrophobic surface. Thus NaCl or KCl can be floated with air bubbles.

As discussed by many researchers, for soluble-salt flotation, amine collector precipitation is significant. The results from this research indicate that DDM collector



precipitation also plays an important role in a morpholine flotation system.

The nature of interfacial water was preliminarily studied using MD simulation. The water-density profile analysis from MDS indicated that water structure depends on the salt solution. Interfacial water at a NaCl surface has a parallel hydrogen/oxygen configuration. At the surface of KCl, interfacial water has a hydrogen/oxygen/hydrogen configuration due to the increasing cation size. The water residence time at an NaCl surface, about 30 ps, is longer than at a KCl surface, 20 ps. This means that interfacial water is more stable at an NaCl surface than at a KCl surface. However, compared with carnallite's, these water residence times are very short. Since the carnallite surface is completely hydrated, collector molecules or the collector colloid cannot replace interfacial water molecules. Thus carnallite particles maintain hydrophilic status during flotation.

## REFERENCES

- Berendsen, H. J. C., Grigera, J. R., and Straatsma, T. P., 1987, "The Missing Term in Effective Pair Potentials," *J. Phys. Chem.* **91**, pp. 6269-6271.
- Cao, Qinbo, 2010, "Surface Chemistry Features in the Flotation of KCl," *Minerals Engineering* **23**, pp. 365–373
- Du, H. and Miller, J. D., 2007, "Interfacial Water Structure and Surface Charge of Selected Alkali Chloride Salt Crystals in Saturated Solutions: A molecular dynamics modeling study," *J. Phys. Chem. C* **111** (27), pp. 10013–10022.
- Du, H., Liu, J., Ozdemir, O., Nguyen, A. V., and Miller, J. D., 2008, "Molecular Features of the Air/Carbonate Solution Interface," *J. Colloid and Interface Science* **318**, pp. 271–277.
- Fuerstenau, D. W., and Fuerstenau, M. C., 1956, "Ionic Size in Flotation Collection of Alkalihalides," *Transactions of the American Institute of Mining, Metallurgical and Petroleum Engineers* (Tech. Publ. 4156-B), p. 205
- Gruner, J. W., 1934, "The Crystal Structures of Talc and Pyrophyllite," *General and Physical Chemistry* (Section 2), CODEN: ZKKKAJ; ISSN: 044-2968.
- Hancer, M., Celik, M. S., and Miller, J. D., 2001, "The Significance of Interfacial Water Structure in Soluble Salt Flotation Systems," *Journal of Colloid and Interface Science* **235** (1), pp. 150–161.
- Hancer, M., and Miller, J. D., 2000, "The Flotation Chemistry of Potassium Double Salts: Schoenite, kainite, and carnallite," *Minerals Engineering* **13** (14–15), pp. 1483–1493.
- Jin, Jiaqi, 2012, Department of Metallurgical Engineering, University of Utah, work in progress.
- Laskowski, J. S., Yuan, X. M., and Alonso, E. A., 2008, "Potash Ore Flotation – How does it work?" In: *Proc. 24th Int. Mineral Processing Congress*, Beijing, pp. 1270–1276.

- Miller, J. D., Yalamanchili, M. R., and Kellar, J. J., 1992, "Surface Charge of Alkali Halide Particles as Determined by Laser-Doppler Electrophoresis," *Langmuir* **8** (5), pp. 1464–1469.
- Perdikatsis, B., and Burzlaff, H., 1981., Strukturerfeinerung am Talk. *Zeitschrift für Kristallographie* **156**, pp. 177–186.
- Perucca, C. F., 2003, "Potash Processing in Saskatchewan: A review of process technologies," *CIM Bulletin* **96** (1070), pp. 61-65.
- Perucca, C.F., Potash processing in Saskatchewan- a review of process technologies. *CIM Bulletin* 96 No.1070, 2003
- Randall T. Cygan, Jian-Jie Liang, and Andrey G. Kaliniche, 2004, "Molecular Models of Hydroxide, Oxyhydroxide, and Clay Phases and the Development of a General Force Field," *Journal of Physical Chemistry B* **108**, pp. 1255-1266.
- Rogers, J., 1957, "Flotation of Soluble Salts," *Institution of Mining and Metallurgy Bulletin* **607**, pp. 439–452
- Rogers, J., and Schulman, J. H., 1957. Mechanism of the selective flotation of soluble salts in saturated solutions. In: *Proc. 2nd Intern. Congr. Surface Activity*, London, vol. 3, pp. 243–251 (discussion 372-5).
- Roman, R. J., Fuerstenau, M. C., and Seidel, D. C., 1968, "Mechanisms of Soluble Salt Flotation. I.," *Transaction of the American Institute of Mining, Metallurgical and Petroleum Engineers* **241** (1), pp. 56-64.
- Searls, J. P., 1990, *Minerals Year Book – 1989*, p. 801.
- Titkov, S., Sabirov, R. and Panteleeva, N., 2003, "Investigations of Alkylmorpholines—Collectors for a new halite flotation process," *Mineral Engineering* **16**, pp. 1161-1166.
- U. S. Geological Survey, 2012, *Mineral commodity summaries 2012*: U. S. Geological Survey, p. 122
- Wang, Lijuan, Liu, Gousheng, Song, Xingfu, and Yu, Jian Guo, 2009, "Molecular Modeling for Selective Adsorption of Halite with Dodecylmorpholine," *Acta Phys. Chim. Sin. (China)* **25** (5) pp. 963–969.
- Yalamanchili, M. R., Kellar, J. J., and Miller, J. D., 1993, "Adsorption of Collector Colloids in the Flotation of Alkali Halide Particles," *International Journal of Mineral Processing* **39** (1-2), pp. 137-153.

- Ye, Y., Khandrika, S. M., and Miller, J. D., 1989, "Induction Time Measurements at a Particle Bed," *International Journal of Mineral Processing* **25**, pp. 221–240.
- Yu, Jianguo, and Song, Xingfu, 2001, "A New Method for Synthesis Dodecyl Morpholine," CN1312247. 2001. 01. 16.
- Zhang, Wanpin, and Song, Xingfu, 2006, "Selective Flotation Mechanism Sodium Chloride Particle with Dodecylmorpholine, *Journal of Chemical Industry and Engineering* (China) **57** (5), pp. 1171-1176.